

MODERN PATHOLOGY

 USCAP 2018

ABSTRACTS

NEUROPATHOLOGY AND
OPHTHALMIC PATHOLOGY
(1812-1862)

107TH ANNUAL MEETING

GEARED
TO LEARN



MARCH 17-23, 2018

Vancouver Convention Centre
Vancouver, BC, Canada

EDUCATION COMMITTEE

Jason L. Hornick, Chair
 Rhonda Yantiss, Chair, Abstract Review Board
 and Assignment Committee
 Laura W. Lamps, Chair, CME Subcommittee
 Steven D. Billings, Chair, Interactive Microscopy
 Shree G. Sharma, Chair, Informatics Subcommittee
 Raja R. Seethala, Short Course Coordinator
 Ilan Weinreb, Chair, Subcommittee for
 Unique Live Course Offerings
 David B. Kaminsky, Executive Vice President
 (Ex-Officio)
 Aleodor (Doru) Andea
 Zubair Baloch
 Olca Basturk
 Gregory R. Bean, Pathologist-in-Training
 Daniel J. Brat

Amy Chadburn
 Ashley M. Cimino-Mathews
 James R. Cook
 Carol F. Farver
 Meera R. Hameed
 Michelle S. Hirsch
 Anna Marie Mulligan
 Rish Pai
 Vinita Parkash
 Anil Parwani
 Deepa Patil
 Lakshmi Priya Kunju
 John D. Reith
 Raja R. Seethala
 Kwun Wah Wen, Pathologist-in-Training

ABSTRACT REVIEW BOARD

Narasimhan Agaram	Mamta Gupta	David Meredith	Souzan Sanati
Christina Arnold	Omar Habeeb	Dylan Miller	Sandro Santagata
Dan Berney	Marc Halushka	Roberto Miranda	Anjali Saqi
Ritu Bhalla	Krisztina Hanley	Elizabeth Morgan	Frank Schneider
Parul Bhargava	Douglas Hartman	Juan-Miguel Mosquera	Michael Seidman
Justin Bishop	Yael Heher	Atis Muehlenbachs	Shree Sharma
Jennifer Black	Walter Henricks	Raouf Nakhleh	Jeanne Shen
Thomas Brenn	John Higgins	Ericka Olgaard	Steven Shen
Fadi Brimo	Jason Hornick	Horatiu Olteanu	Jiaqi Shi
Natalia Buza	Mojgan Hosseini	Kay Park	Wun-Ju Shieh
Yingbei Chen	David Hwang	Rajiv Patel	Konstantin Shilo
Benjamin Chen	Michael Idowu	Yan Peng	Steven Smith
Rebecca Chernock	Peter Illei	David Pisapia	Lauren Smith
Andres Chiesa-Vottero	Kristin Jensen	Jenny Pogoriler	Aliyah Sohani
James Conner	Vickie Jo	Alexi Polydorides	Heather Stevenson-Lerner
Claudiu Cotta	Kirk Jones	Sonam Prakash	Khin Thway
Tim D'Alfonso	Chia-Sui Kao	Manju Prasad	Evi Vakiani
Leona Doyle	Ashraf Khan	Bobbi Pritt	Sonal Varma
Daniel Dye	Michael Kluk	Peter Pytel	Marina Vivero
Andrew Evans	Kristine Konopka	Charles Quick	Yihong Wang
Alton Farris	Gregor Krings	Joseph Rabban	Christopher Weber
Dennis Firchau	Asangi Kumarapeli	Raga Ramachandran	Olga Weinberg
Ann Folkins	Frank Kuo	Preetha Ramalingam	Astrid Weins
Karen Fritchie	Alvaro Laga	Priya Rao	Maria Westerhoff
Karuna Garg	Robin LeGallo	Vijaya Reddy	Sean Williamson
James Gill	Melinda Lerwill	Robyn Reed	Laura Wood
Anthony Gill	Rebecca Levy	Michelle Reid	Wei Xin
Ryan Gill	Zaibo Li	Natasha Rekhman	Mina Xu
Tamara Giorgadze	Yen-Chun Liu	Michael Rivera	Rhonda Yantiss
Raul Gonzalez	Tamara Lotan	Mike Roh	Akihiko Yoshida
Anuradha Gopalan	Joe Maleszewski	Marianna Ruzinova	Xuefeng Zhang
Jennifer Gordetsky	Adrian Marino-Enriquez	Peter Sadow	Debra Zynger
Ilyssa Gordon	Jonathan Marotti	Safia Salaria	
Alejandro Gru	Jerri McLemore	Steven Salvatore	

To cite abstracts in this publication, please use the following format: **Author A, Author B, Author C, et al. Abstract title (abs#). *Modern Pathology* 2018; 31 (suppl 2): page#**

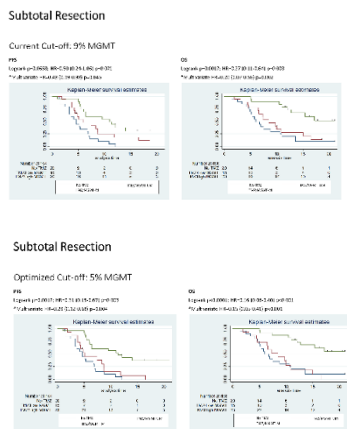
1812 MGMT Promoter Methylation Status in Glioblastoma: A single Institutional Experience

Abdullah T Almuqate¹, Wajid Sayeed², Elizabeth Kornaga³, Ana Nikolic², Gloria B Roldan-Urgoit⁴, Doha Itan⁵. ¹University of Calgary, Calgary, AB, ²University of Calgary, ³Alberta Health Services, ⁴Tom Baker Cancer Centre, University of Calgary, Calgary, AB, ⁵Calgary Laboratory Services/University of Calgary, Calgary, AB

Background: O6-methylguanine-DNA methyltransferase promoter methylation (mMGMT) in Glioblastoma (GB) is a predictive indicator of better survival and responsive to temozolomide (TMZ). Clinically, TMZ is used for all patients with good performance status irrespective of mMGMT due to observed benefit in some patients with unmethylated tumors. A 9% mMGMT cut-off was analytical validated for a Methylation-specific restriction enzyme quantitative PCR. We aim to evaluate the current cut-off in context of patient outcomes and to query a cut-off with more clinical relevance.

Design: Cases of GB tested for mMGMT in 2015 and 2016 were retrieved from the database of the Molecular Diagnostic Laboratory. Relevant clinical parameters were collected including patients' demographics, extent of surgical resection, progression free survival - PFS, overall survival - OS, and percentage of mMGMT. Cox models were adjusted for patient age, sex and surgery.

Results: We retrieved 158 GB cases: 85 males and 73 females with mean age of 61 years. Tissue was obtained by biopsy (14 cases), subtotal resection (ST; 60 cases), and gross total resection (GT; 84 cases). Median OS for biopsy and any surgery in the full cohort was 5 and 15 months, respectively (HR=0.23, p<0.001). Using 9% mMGMT cut-off, the median OS for patients with MGMT methylated tumors (MGMT-M) that received TMZ was >21 months and for those with unmethylated tumors (MGMT-UM) who received TMZ was 14.4 months (HR=0.28, p<0.001). Using an optimized cut-off of 5% mMGMT, the median OS for patients treated with TMZ was >21 months for MGMT-M and 13.9 months for MGMT-UM (HR=0.24, p<0.001). The 5% cut-off improved stratification for PFS and OS for the STgroup (see Figures 1&2) but showed no difference for the GT group.



Conclusions: In our cohort, cases with MGMT-M tumors showed comparable OS for the ST and GT groups. TMZ had little effect on OS in ST patients when the tumor was MGMT-UM (Figures 1 & 2). This group may benefit from de-escalation of therapy with TMZ to avoid side effects. Most patients that benefited from TMZ despite MGMT-UM tumors belonged to the GT group (data not shown). Our next step is to review the H&E slides to evaluate whether the percent of tumor cells in the tissue submitted for mMGMT testing has an impact on cut-off determination in relation to clinical outcome. We plan to expand our cohort in order to improve statistical power and analysis. We also aim to validate our findings in a cohort from another institution.

1813 CITED1 as a Potential Regulator of Metastasis in Uveal Melanoma

Sabrina Bergeron¹, Jade Lasiste², Pablo Zoroquiain³, Tadhg Ferrier⁴, Ana Beatriz Toledo Dias², Miguel Burnier. ¹MUHC - McGill University Ocular Pathology Laboratory, Montreal, QC, ²MUHC-McGill Ocular Pathology Laboratory, ³Montreal, PQ, ⁴MUHC-McGill University Ocular Pathology Laboratory, Montreal, QC

Background: Uveal melanoma (UM) is the most common primary intraocular tumor in adults. Metastatic disease is the leading cause of mortality in these patients. It develops in up to 50% of patients, despite control of the primary tumor and even after years of a

disease-free state known as tumor dormancy. While the mechanisms underlying metastasis in UM remain poorly understood, it is theorized that early in the disease, malignant UM cells enter systemic circulation and preferentially migrate to the liver and lungs. Studies have shown that mesenchymal-to-amoeboid transition (MAT) is the main process by which mesenchymal tumor cells metastasize. The TGFβ-SMAD2-CITED1 axis has been shown to regulate MAT in cutaneous melanoma. This study therefore aims to assess the expression of CITED1 in uveal melanoma and its association with clinicopathological features.

Design: Twenty-two cases of UM were retrieved from the ocular pathology laboratory archive. Automated immunohistochemistry for CITED1 was performed, and whole digital slides were acquired using the Philips IntelliSite scanner. Clinicopathologic features, such as age at diagnosis, tumor dimension, prior radiation treatment, follow-up and immunoreactivity scores (IRS; % of positive cells x intensity) for CITED1 were evaluated for all cases. Statistical correlations were performed using the SPSS software.

Results: CITED1 was expressed in 100% of malignant cells, regardless of prior radiation treatment (5/22 cases) and tumor dimension (mean: 12 mm). Kaplan-Meier survival curves using the Log-rank test showed a positive correlation between CITED1 IRS and the occurrence of metastasis (p=0.04). In contrast, normal choroidal melanocytes adjacent to the tumor did not express CITED1.

Conclusions: Our results demonstrate an association between higher CITED1 expression in UM and a greater risk of metastatic disease. Moreover, the lack of correlation between levels of CITED1 expression and tumor dimensions suggests that CITED1 is not directly linked to growth of the tumor.

The expression of CITED1 only in malignant melanocytes proposes a possible mechanism by which tumor cells may undergo MAT prior to entering the systemic circulation. Further *in vitro* characterization of CITED1 regulated tumor evasion in uveal melanoma is required to support this hypothesis.

1814 High Grade Gliomas Involving The Subventricular Zone - A Molecular Study of 32 cases

Aden K Chan¹, Riki R Zhang², Ho Keung Ng³. ¹The Chinese University of Hong Kong, Shatin, New Territories, ²The Chinese University of Hong Kong, ³Prince of Wales Hosp, Shatin

Background: High grade gliomas abutting on the subventricular region have been described to show aggressive features and poor outcomes but there has been no detailed study of the molecular features of these tumors.

Design: We studied 32 such tumors from our archives, all except one being glioblastomas, for their clinical features and tested them for amplification of *c-myc*, *MYCN*, *EGFR*, mutations of *H3F3A-K27M*, *TERTp*, *IDH1-R132H*, deletion of 10q, and by immunohistochemistry ATRX, nestin and SOX2.

Results: *c-Myc* and *MYCN* were each amplified in 32.3% of cases and together were amplified 58% of the cases. This is in contrast to information derived from known TCGA glioblastoma data set where *c-Myc* and *MYCN* were only rarely amplified in glioblastoma. *MYCN* in addition was associated with younger age (p=0.029), concomitant *H3F3A-K27M* mutation (p=0.002), non-amplified *EGFR* (p=0.023) and mid-line location (p=0.012). Interestingly, we found a low percentage of *TERTp* mutation (19%) among these high grade gliomas which was mutually exclusive with a higher frequency of loss of ATRX expression (p=0.025). The majority (91%) of tumors were *IDH* wild type and 39% of them were deleted for 10q. Moreover, 97% of cases expressed at least one of the stem cell markers, which may be related to the supposedly subventricular location of neural stem cells. 89% of cases relapsed with 50% showing CSF dissemination. However, there was no statistical relationship between survivals and biomarkers or other clinical parameters.

Conclusions: In conclusion, our study has identified a subgroup of subventricular zone high grade gliomas characterized by *c-Myc*, *MYCN* amplification and frequent expression of stem cell markers and a high rate of CSF dissemination.

1815 Decreased CIC and FUBP1 Expressions Are Associated with Poor Prognosis in Anaplastic Astrocytomas

Yen-Ying Chen¹, Chih-yi Hsu². ¹Taipei City, ²Taipei Veterans General Hospital, Taipei, Taiwan

Background: Mutations of CIC (homolog of *Drosophila capicua*) and FUBP1 (far upstream element binding protein 1) genes, located respectively on 19q13 and 1p31, have been detected frequently in oligodendrogliomas and less commonly in astrocytomas. Absent CIC and FUBP1 expressions have been shown to associate with shorter time to recurrence in oligodendroglial tumors, but their prognostic impacts on astrocytic tumors have not been examined. This study aims to investigate the expression patterns and prognostic values of CIC and FUBP1 in anaplastic astrocytomas.

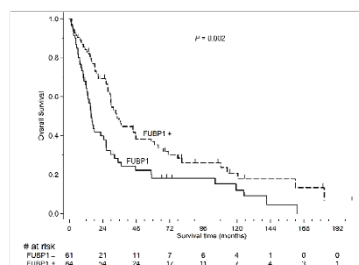
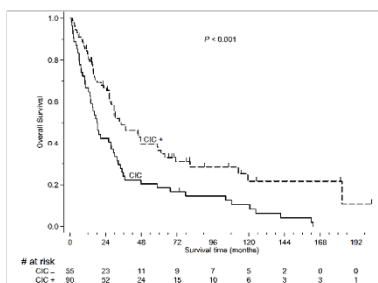
Design: One hundred and forty-five patients with primary anaplastic astrocytomas who had adequate follow-up data were included in the study. The expressions of CIC and FUBP1 were evaluated by immunohistochemistry. The results were correlated with the survival of the patients.

Results: Decreased CIC and FUBP1 protein expressions, defined as <50% of tumor cells staining, were identified in 37.9% (55/145) and 42.1% (61/145) of anaplastic astrocytomas, respectively. The 1p and 19q status evaluated by fluorescence in situ hybridization was not significantly associated with the protein expression for both genes. Decreased CIC and FUBP1 expressions were significantly associated with shorter overall survival ($p < 0.001$ and $p = 0.002$, respectively). Their impact on survival remained statistically significant in the multivariate analyses with adjustment of age, gender, extent of resection, bevacizumab/temozolomide treatment, IDH1/2 mutation status and ATRX expression ($p = 0.002$ and $p = 0.013$ for CIC and FUBP1, respectively).

Table 1. Median survival time and multivariate survival analyses by the expression of CIC and FUBP1

	N (%)	Median survival (mo)	P	Hazard ratio*	P
CIC < 50%	55 (37.9)	18.5	< 0.001	1	0.002
CIC ≥ 50%	90 (62.1)	34.3		0.430	
FUBP1 < 50%	61 (42.1)	15.7	0.002	1	0.013
FUBP1 ≥ 50%	84 (57.9)	34.3		0.533	

* The influences of age, gender, extent of resection, bevacizumab treatment, temozolomide treatment, IDH1/2 mutation and ATRX were adjusted.



Conclusions: Our results suggest that decreased CIC and FUBP1 expressions can serve as prognostic markers of shorter survival in patients with anaplastic astrocytoma.

1816 In Situ Hybridization Confirms Overexpression of Novel Potential Therapeutic Target (Hsa-miR-21) In High Grade Gliomas

Jinjun Cheng¹, Yongchao Li², Blazej Zbytek³, Krishan Kalra⁴, Mahul Amin⁵, Lawrence M Pfeffer⁶. ¹Memphis, TN, ²The University of Tennessee Health Science Center, ³Pathology Group/Mid-south, Germantown, TN, ⁴BioGenex Laboratories, ⁵Methodist University Hospital, Memphis, TN, ⁶The University of Tennessee Health Science Center, Memphis, TN

Disclosures: Krishan Kalra: *Research Support*, BioGenex

Background: Hsa-mir-21 is the most frequently overexpressed microRNA in glioblastoma and many other human cancers. Our previous studies show that high miR-21 expression is associated with high proliferation, low apoptosis, high invasion and metastatic potential of multiple cancer cells and promotes oncogenesis. MicroRNA in situ hybridization has been approved to efficiently detect in situ expression of miRNA within FFPE tissue. Here we investigated in situ expression of miR-21 within low or high glioma as well as normal brain tissue and explored its potential diagnosis role.

Design: We selected 24 cases of high-grade gliomas, 14 cases of low-

grade gliomas and 14 cases of autopsy brain cortex without gross pathological changes and incorporated representative tissue (1mm in diameter) into a tissue microarray. In situ hybridization staining performed on Xmatrx automated system using FAM-labeled miRNA probes (BioGenex, CA) for miR-21 was performed on tissue array. The H&E quality and in situ hybridization results were independently reviewed by two pathologists. The hybridization intensity, percentage of positive cells, identity of positive cells were documented and analyzed.

Results: miR-21 shows variable weak hybridization (including cytoplasmic and nuclear) in normal human organ tissue. In our high grade glioma cohort, 60% of gliomas show intense nuclear staining in more than 90% of tumor cells and the remaining 40% show moderate to intense nuclear stain in at least 50% tumor cells. In contrast, miR-21 shows variable hybridization pattern in low grade gliomas and normal brain tissue. Representative results of miR-21 in situ hybridization is shown in Figure 1. Interestingly, endothelial cells within both low and high grade glioma show moderate to intense miR21 expression.

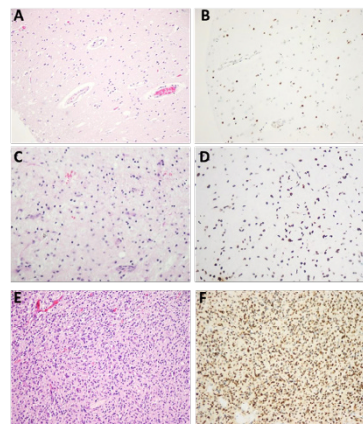


Figure 1. A and B. Scattered nuclear and cytoplasmic stain on neurons, microglia, and astrocytes in autopsy brain cortex. C and D. Moderate to intense nuclear staining in low grade glioma cells; Majority of endothelial cells within gliomas are also moderately to intensely stained. E and F. Intense nuclear staining on more than 90% high grade glioma cells and endothelial cells within tumor.

Conclusions: In the current study, we confirmed the overexpression of miR-21 by in situ hybridization in FFPE high grade glioma tissue. Our study also provided experimental evidence of the importance of miR-21 expression pattern during gliomagenesis. miR-21 can serve as potential actionable target in the therapy of high grade gliomas.

1817 Multiplexed Immunofluorescence Reveals Potential Immune Checkpoint Vulnerabilities in Craniopharyngioma

Shannon Coy¹, Rumana Rashid¹, Jia-Ren Lin³, Ziming Du¹, Peter E Manley³, Mark W Kieran³, David A Reardon³, Peter Sorger², Sandro Santagata¹. ¹Brigham and Women's Hospital, Boston, MA, ²Harvard Medical School, ³Dana Farber Cancer Institute, Boston, MA

Disclosures: Peter Sorger: *Advisory Board*, RareCyteScientific; *Stock*, RareCyteScientific, Glencoe Inc.

Background: Craniopharyngiomas are epithelial neoplasms of the sellar/parasellar region which are hypothesized to arise from developmental derivatives of the stomodeal ectoderm and Rathke's pouch. Adamantinomatous craniopharyngiomas (ACP) occur in all age groups, whereas papillary craniopharyngiomas (PCP) occur almost exclusively in adults. Craniopharyngiomas have excellent long-term survival, but both subtypes are associated with profound morbidity including hypothalamic and endocrine dysfunction, which are often exacerbated by surgery, and recurrences are common. BRAF V600E mutations in PCP render them susceptible to BRAF/MEK inhibitors, but effective targeted therapies are not available for ACP.

Design: We quantified and mapped PD-L1 and PD-1 expression in 23 ACP and 18 PCP resection specimens using immunohistochemistry and immunofluorescence and confirmed expression with RNA in situ hybridization. We used multiplexed cyclic immunofluorescence (CyCIF) to map the spatial distribution and density of immune infiltrates and characterized cell cycle and signaling pathways in ACP tumor cells with intrinsic expression of PD-1.

Results: All adamantinomatous (23/23; 100%) and papillary (18/18; 100%) craniopharyngiomas expressed PD-L1. In ACP, PD-L1 was predominantly expressed by tumor cells comprising the cyst lining. In PCP, PD-L1 was highly-expressed by tumor cells surrounding stromal/fibrovascular cores. ACP also invariably showed membranous tumor cell intrinsic PD-1 expression in whorled epithelial cells with nuclear-translocated beta-catenin. These cells exhibited increased pERK and pS6, suggestive of activation of intracellular signaling downstream of PD-1. Cells with membranous PD-L2 expression were identified in close association with the PD-1 positive whorls. Quantitative and spatial profiling of immune populations showed a modest density of tumor infiltrating CD8+ cytotoxic T cells, low densities of PD-L1+

macrophages and FOXP3+ regulatory T-cells, and enrichment of immune populations in the peritumoral/stromal compartment.

Conclusions: ACP exhibit intrinsic PD-L1 expression in the tumor cyst lining and intrinsic PD-1 expression in the proposed oncogenic stem-like population of whorled epithelial cells with nuclear-translocated beta-catenin. In PCP, proliferative basally oriented tumor cells strongly express PD-L1 in a continuous band at the stromal-epithelial interface. Targeting PD-L1 and/or PD-1 in both subtypes of craniopharyngioma might therefore be a valuable therapeutic strategy.

1818 Grading Considerations for Meningeal Solitary Fibrous Tumor/Hemangiopericytoma

Karen Fritchie¹, Sarah M Jenkins², Fausto Rodriguez³, Andrew Guajardo⁴, Arie Perry⁵, Ashley Wu⁶, Sandro Santagata⁷, Alexander B Kaplan⁸, Sabrina Ross⁹, Michael Link¹⁰, Paul Brown¹⁰, Kassandra Jensch¹¹, Florian Haller¹², Priscilla Brastianos¹³, David Louis¹⁴, Brian Alexander¹⁵, David Raleigh¹⁶, Jose Velázquez Vega¹⁷, Fabio Ferrarese¹⁸, Daniel Braß¹⁹, Caterina Giannini¹. ¹Mayo Clinic, Rochester, MN, ²Mayo Clinic Rochester, ³Johns Hopkins Univ, Baltimore, MD, ⁴Baltimore, MD, ⁵Univ. of California, SF Pathology Div Of Neuropath, San Francisco, CA, ⁶UCSF, San Francisco, CA, ⁷Brigham and Women's Hospital, Boston, MA, ⁸MGH, Boston, MA, ⁹Treviso General Hospital, Treviso, Treviso, ¹⁰Mayo Clinic, ¹¹University Hospital Erlangen, Erlangen, Bavaria, ¹²Erlangen, Germany, ¹³MGH, ¹⁴Massachusetts General Hospital, Boston, MA, ¹⁵Harvard, ¹⁶UCSF, ¹⁷Emory, ¹⁸Hospital Treviso, ¹⁹Northwestern University Feinberg School of Medicine, Chicago, IL

Background: Meningeal solitary fibrous tumor (SFT) and hemangiopericytoma (HPC), unified in the WHO 2016 CNS tumor classification, are currently classified by a 3-tier system based on both histopathologic phenotype and mitotic count, whereas malignancy in soft-tissue based SFT is determined by >4 mitoses per 10 HPFs (WHO 2013).

Design: We studied a cohort of 139 patients (63F, 76M; mean age 53 years [range 20-87]) with meningeal SFT/HPC, pathologically confirmed through review of the first tumor resection (n=101), local recurrence (n=37) or distant metastasis (n=1). A STAT6 immunostain showed nuclear expression in 133 (of 139). We recorded the histopathologic phenotype (SFT vs HPC vs intermediate), mitotic count (per 10 HPF) and necrosis. Based on these features, tumors were classified and graded according to the WHO classification of CNS tumors (2016) (grade 1,2 or 3) or Soft Tissue tumors (2013) (SFT or malignant SFT). Clinical follow-up was obtained through chart review. Recurrence-free and overall survivals were evaluated.

Results: The histopathologic phenotype was SFT (n=56), HPC (n=27) or intermediate (n=56). Mitotic count median was 2 with interquartile range (min-max) 1,6 (0-45). Necrosis was present in 17 cases (12%). Recurrence-free and overall survival at 10 years were respectively 73% (95% CI:65-82) and 65% (95% CI:52-77). 39 patients had at least 1 recurrence after their baseline date, 9 had metastases and 2 both. 32 patients died. On univariate analysis WHO CNS and Soft Tissue grade were significantly associated with recurrence-free (p-value respectively 0.015 and 0.0039) but not overall survival, as was necrosis (p=0.0013). Recurrence-free survival at 10 years was respectively 59.4, 54.9 and 32.1% for CNS WHO grade 1,2 and 3 versus 55.9 and 32.1% for Soft Tissue WHO SFT and malignant SFT. Recurrence-free survival at 10 years was respectively 0% and 53.3% for tumors with and without necrosis.

Conclusions: SFT/HPC is a tumor with high frequency of recurrence and a tendency to metastasize. Grading is significantly associated with recurrence-free but not overall survival. In both grading schemes, SFT/HPC can be stratified into two grades, with the additional WHO CNS grade not appearing to be of prognostic significance. The importance of necrosis as a grading criteria needs to be further explored.

1819 Comprehensive Genomic Profiling of Relapsed and Refractory Choroid Plexus Tumors of the Central Nervous System

Kristyn M Galbraith¹, Shakti Ramkissoon², Laurie Gay³, Julia A Elvin⁴, James Suh⁵, Eric Severson⁶, Sugganth Daniel⁷, Siraj Ali⁸, Alexa B Schrock⁹, Jon Chung¹⁰, Vincent A Miller¹, Philip M Stephens², Jeffrey S Ross, Robert Corona¹⁰. ¹SUNY Upstate Medical University, ²Foundation Medicine, Morrisville, NC, ³Foundation Medicine, Cambridge, MA, ⁴Foundation Medicine, Inc, Cambridge, MA, ⁵Foundation Medicine, Inc., Morrisville, NC, ⁶Foundation Medicine, Inc, Morrisville, NC, ⁷Foundation Medicine, Cambridge, MA, ⁸Cambridge, MA, ⁹Foundation Medicine, Cambridge, MA, ¹⁰SUNY Upstate Medical Univ, Syracuse, NY

Disclosures:

Shakti Ramkissoon: *Employee*, Foundation Medicine, Inc.
Laurie Gay: *Employee*, Foundation Medicine, Inc.
James Suh: *Employee*, Foundation Medicine, Inc.
Eric Severson: *Employee*, Foundation Medicine, Inc.
Siraj Ali: *Employee*, Foundation Medicine, Inc.
Alexa Schrock: *Employee*, Foundation Medicine, Inc.
Jon Chung: *Employee*, Foundation Medicine, Inc.

Philip Stephens: *Employee*, Foundation Medicine, Inc.
Jeffrey Ross: *Employee*, Foundation Medicine, Inc.

Background: Choroid plexus tumors (CPT) are rare primary CNS tumors that include the WHO Grade 1 papilloma (CPP), the Grade 2 atypical papilloma (ACPP) and the Grade 3 carcinoma (CPC). In this study, we used a hybrid capture based comprehensive genomic profiling assay (CGP), to define the genomic alterations (GA) in clinically aggressive CPT and correlated the findings with clinicopathologic variables.

Design: DNA was extracted from 40 microns of FFPE specimen from 27 cases of relapsed, refractory CPT. CGP was performed using a hybrid-capture, adaptor ligation based next generation sequencing assay to a mean coverage depth of 630X. Tumor mutational burden (TMB) was determined on 1.1 Mbp of sequenced DNA and microsatellite instability (MSI) was determined on 114 loci. The results were analyzed for all classes of genomic alterations (GA), including base substitutions, insertions and deletions (short variants; SV), fusions, and copy number changes including amplifications (amp) and homozygous deletions.

Results: Clinicopathologic features and GA results are shown in the Table. CPP had a low Ki67 index, low 0.7 GA/tumor, absent oncogene (OG) and tumor suppressor (TS) and TMB, but featured significant *TERT* mutations suggesting methylation silencing events. The ACPP had an intermediate Ki67 index and 1.5 GA/tumor with intermediate frequencies of OG activation and TS loss, 27% *TERT* GA, but low TMB. The CPC featured significantly higher Ki67 indices, higher 2.67 GA/tumor, 0% *TERT* GA with intermediate OG activation but high TS loss at 75% and including 45% of cases with *TP53* GA, but 0% of cases with high TMB. Clinically relevant (actionable) GA in all 3 groups were relatively rare, but included targets such as *MET*, *EGFR*, *KIT* and *PTEN* in less than 20% of the sequenced CPT. No CPT featured MSI-High status.

GA	CPP Grade 1	Atypical CPP Grade 2	CPC Grade 3
Cases	3	11	12
Median Age (years)	34	13	51
Gender	M 66%	M 55%	M 50%
Epithelial Marker +*	100%	83%	91%
Mean Ki-67 Index#	2%	8%	30%
GA/tumor	0.7	1.5	2.67
Oncogene Activation	0%	27%	25%
Tumor Suppressor Gene Loss	0%	18%	75%
TP53	0	0	45%
TERT	33%	27%	0%
MSI-High Status	0%	0%	0%
TMB ≥ 20 mut/Mb	0%	0%	0%

Conclusions: CGP can identify significant differences in GA among the 3 groups of recurrent/refractory CPT reflecting the contrasting histologic appearances of the low, intermediate and high grade nature of the groups. Given the low TMB and absence of MSI, opportunities for immunotherapies for the CPT patients appear limited, but a minority CPT harbor potentially targetable GA that could potentially impact clinical outcome.

1820 Epithelial differentiation with microlumen formation in meningioma – diagnostic utility of NHERF1/EBP50 immunohistochemistry

Maria-Magdalena Georgescu¹, Adriana Olariu², Bret Moblely³, Phyllis Faust⁴, Jack Raisanen⁵. ¹Louisiana State University/Shreveport, Shreveport, LA, ²Medical University of South Carolina, Charleston, SC, ³Vanderbilt University, Nashville, TN, ⁴Columbia University, ⁵University of Texas Southwestern, Dallas, TX

Background: Meningioma is a primary brain tumor arising from the neoplastic transformation of meningeothelial cells. Thirteen histological variants of meningioma are recognized. Here we show that NHERF1/EBP50, an adaptor protein required for structuring specialized polarized epithelia, can distinguish meningioma variants with epithelial differentiation.

Design: The study assembled 92 brain tumor cases from various institutions across the country, including 80 meningiomas (12 WHO grade I most common variants, 11 secretory, 23 chordoid, 8 tumors with chordoid component, 2 clear cell, 20 atypical WHO grade II, 4 anaplastic WHO grade III). Demographic data include age, gender and location for all cases, and survival for the chordoid meningioma cases. IHC for NHERF1 was performed for all the cases, and for NF2, moesin, EMA and progesterone receptor for the meningiomas. Electron microscopy was performed on 3 cases. Statistical analysis of the demographic data and densitometry was performed.

Results: NHERF1 decorates the membrane of intracytoplasmic lumens and microlumens in the secretory variant, consistent with a previously described epithelial differentiation of this subtype. NHERF1 also labels microlumens in chordoid meningioma, an epithelial variant not previously known to harbor these structures. Ultrastructural analysis confirmed the presence of microlumens with microvilli projecting into the lumen. NHERF1 associates with the ezrin-radixin-moesin (ERM)-NF2 cytoskeletal proteins, and moesin but not NF2 was detectable in the microlumens. NHERF1 revealed microlumens in 87% of the chordoid meningioma and meningioma with chordoid component cases, and in 100% of the secretory meningioma cases. The most common WHO grade I meningioma variants lacked microlumens. Interestingly, 25% and 75% of WHO grades II and III meningiomas, respectively, showed microlumen formation, mainly in papillary-like or sheeting areas, revealing a new subset of high grade meningiomas with epithelial differentiation. NHERF1 failed to detect microlumens in chordoid glioma of the 3rd ventricle, chordoma and chondrosarcoma, conditions that sometimes share similar histological appearance to chordoid meningioma.

Conclusions: This study uncovers features of epithelial differentiation in meningioma and proposes NHERF1 as new stain for the differential diagnosis of chordoid meningioma.

1821 Histology of the Filum Terminale in Pediatric Tethered Cord Syndrome – Study of 114 Consecutive Cases

Mercia Gondim, Laurie Ackerman, Daniel Fulkerson, Jose M Bonnin, Alexander O Vortmeyer. Indiana University School of Medicine, Indianapolis, IN

Background: Tethered cord syndrome (TCS) is a functional disorder of the distal spinal cord leading to traction of distal cord elements. The current treatment is surgical transection of the filum terminale (FT). Multiple studies have described the histology and embryology of the normal FT. However, literature on the histology of the FT in pediatric TCS is scarce. We analyzed the histology of the FT in 114 consecutive cases of pediatric TCS.

Design: We retrospectively analyzed cases from TCS surgeries performed in the same institution over a 2.5 year period (January 2015 to July 2017). We reviewed the H&E slides by light microscopy and looked for presence/absence of fat, fibrovascular tissue, nerve bundles and ependymal tissue. In addition, we semiquantitatively assessed the proportion of different histologic elements. We divided the patients according to age, into seven groups: <1-year-old, 1-2-year-old, 2-3-year-old, 4-5-year-old, 6-7-year-old, 8-9-year-old, and 10-16-year-old.

Results: We identified 114 cases. The mean patient age was 5.2 years (range 3 months-16 years); 67 (59%) of the patients were females. Fibrovascular tissue was consistently present and associated with variable amounts of fat (57% of cases). Small amounts of ependymal tissue were variably present (32% of cases). Presence of nerve bundles was frequently seen (91%). The presence of fat was more frequently observed in young patients (0-4 years). In individual biopsies, the proportion of fat shows marked variation, ranging from 0-95%, and was higher in young patients (0-7 years). The frequency of ependymal tissue was 46% in young patients (0-9 years), but rare in older patients (10-16 years).

Conclusions: In agreement with previous studies, we confirm the variable presence of fat, nerve bundles, and ependymal tissue in TCS specimens. Correlating the findings with age, adipose tissue is found more frequently and with a higher proportion in young patients. We conclude that the high proportion of fat within the FT is associated with earlier clinical symptoms and earlier surgical intervention. The findings also suggest that TCS may be related to pathological persistence of fetal adipose tissue resulting in hamartomatous accumulation of adipose tissue. This would concur with existent mechanical hypotheses proposing restricted flexibility/adjustability of the FT during development.

1822 Prion Protein Expression in the Human Retina: A Retrospective Study of 10 Cases

Vanessa S Goodwill¹, Jonathan Lin², Christina Sigurdson³, Henry Sanchez⁴, Michael D Geschwind⁵. ¹University of California, San Diego, San Diego, CA, ²UC-San Diego, La Jolla, CA, ³University of California, San Diego, ⁴University of California, San Francisco, ⁵University of California, San Francisco, San Francisco, CA

Background: Human spongiform encephalopathies, also known as prion diseases, are a rare group of infectious, heritable, and acquired diseases leading to rapid cognitive decline. Prion diseases are considered a serious public health threat due to the high level of infectivity and delayed presentation. Up to 50% of patients with prion disease develop visual symptoms during their clinical course, possibly secondary to abnormal prion protein (PrP^{Sc}) accumulation within the eye. Few studies, however, have investigated the presence of PrP^{Sc} within the eye of patients with sporadic Creutzfeldt-Jakob

disease (sCJD). Knowing the presence of PrP^{Sc} in the eye is important to assess the potential risk of transmission from common ophthalmic surgical procedures. Additionally, the current gold standard of diagnosis remains brain autopsy. If PrP^{Sc} expression is present in the eye, ocular imaging modalities with PrP^{Sc}-binding compounds may enable earlier diagnosis. Here, we investigate the expression of PrP^{Sc} within retinas of confirmed prion disease cases collected from post-mortem enucleations.

Design: From December 2015 to May 2017, 20 eyes were collected from 10 autopsies of clinically suspected prion disease and 6 of non-prion disease at a single institution. sCJD was confirmed in all cases by brain autopsy and genetic analysis of the *PRNP* gene. Immunohistochemistry was performed with antibodies against PrP and PrP deposition within the retina was evaluated and compared with normal controls. Subjects included both male and female patients with ages ranging from 57–80 years old. The clinical disease course ranged from 3–20 months.

Results: In all ten prion disease cases, PrP^{Sc} deposits were observed in the retina by immunohistochemistry. PrP^{Sc} was limited to the outer and inner plexiform layers of the retina and was most prominent in the outer plexiform layer, with the majority of cases exhibiting coarse, 5-10 um well-aligned ovoid deposits. In the sclera, cornea, lens, and optic nerve, no deposits were observed.

Conclusions: PrP^{Sc} deposits were present consistently in the retina of patients with prion disease and can be detected immunohistochemically. Our findings confirm previous isolated reports of retinal PrP^{Sc} expression in the largest series of documented prion cases to date. We suggest that the retina potentially serves as a diagnostic target in clinically suspected prion disease. Additionally, retinal involvement may contribute to visual symptoms commonly associated with prion disease.

1823 Role of next-generation sequencing in vitreoretinal lymphomas (VRL): A new approach to targeted therapies and disease monitoring

Michael Greenwood¹, Reem Alrabeh¹, April Ewton¹, Patricia Cheves-Barrios¹, Jessica Thomas¹, Randall Olsen¹. ¹Houston Methodist Hospital, Houston, TX

Background: Next generation sequencing (NGS) is an established technology which is currently being used for diagnostic and therapeutic purposes in myeloid and lymphoid neoplasms. Vitreoretinal lymphomas (VRL) are a rare form of primary CNS lymphoma. Prognosis is generally poor and outcomes can include loss of vision, CNS involvement, local, and systemic recurrences. Optimal therapy is uncertain and usual therapeutic options include external beam radiation and local and systemic chemotherapy. Targeted novel therapies may better treat or control this type of lymphoma. We report our experience using small-volume vitreous fluid biopsies for NGS of VRL.

Design: We collected diluted and undiluted vitreous specimens from 3 patients with VRL. DNA extractions were performed on 50 microl of specimen and subjected to the 54 gene TruSight DNA Amplicon Myeloid Sequencing. A minimum of 100x read depth coverage is required at a given base for the interpretation of wild-type or variant. The limit of detection is 10% mutant alleles at 100X coverage. Variants are determined relative to the reference human genome hg19. Cytological analysis was performed with immunohistochemical confirmation.

Results: The corresponding cytological diagnosis was that of diffuse large B cell lymphoma (DLBCL) in all three patients. Using NGS, we identified variants in two of the three patient. In patient #1's sample, MYD88 Leu265Pro was present. This is a known somatic gain-of-function mutation that is potentially targetable. It is frequently associated with decreased overall survival and a prognosis similar to ABC type DLBCL. Patient #1's sample also had a DNMT3A variant. Patient #2's sample (Cyclin D1-positive DLBCL) had 3 TP53 variants (Val216Ala, Asn131Ile, and Ser99Phe) which are confirmed somatic mutations and are associated with poor prognosis. TP53 mutated B cell lymphomas can potentially be targeted by Ibrutinib. In addition, several other variants were identified involving DNMT3A, CBL, and KRAS. Patient #3 had no identifiable mutations.

Conclusions: We have demonstrated the feasibility of performing a basic NGS panel on very small-volume vitreous fluid biopsies in vitreoretinal lymphomas. While more studies are needed, this approach can potentially provide valuable information that can be utilized for supporting diagnosis, prognostication, therapeutic targeting and disease monitoring.

1824 Cell cycle regulators as biomarkers of meningioma recurrence: An example with the analysis of CDKN2A (p16) alteration patterns

Anne Guyot¹, Karine Durand², Sandrine Robert², François Caire³, François Labrousse⁴. Limoges Dupuytren University Hospital, ²Limoges Dupuytren University Hospital France, ³CHU Dupuytren, Limoges, Limoges, ⁴Dupuytren University Hospital, Limoges, Limoges

Background: One of the main prognostic factors in meningiomas is the occurrence of a tumor recurrence. According to the WHO classification, aggressive meningiomas show higher mitotic and Ki67 indices than benign ones. Thus, deregulation of the cell cycle could be a mechanism involved in the aggressiveness of some meningiomas. In this study, we investigated somatic molecular alterations of genes regulating the cell cycle.

Design: Using next generation sequencing technique, we studied 84 genes involved in cell cycle regulation in a series of 30 meningiomas, 13 non-recurrent (7 grade I, 5 grade II and 1 grade III) and 17 recurrent (4 grade I, 5 grade II and 8 grade III). Results of the molecular analysis, WHO grade and Ki67 index were analyzed with respect to the presence or not of a tumor recurrence and progression free survival (PFS).

Results: Among the molecular alterations found, the analysis identified in 5 cases, a SNV (Single Nucleotide Variation) on *CDKN2A* gene (NM_000077, exon2, c.G442A, p.Ala148Thr) that was significantly associated with meningiomas recurrence ($p=0.05$). This mutation, confirmed by Sanger sequencing, is referenced in the COSMIC database (Catalog of Somatic Mutations in Cancer) in some other tumors (melanomas, renal clear cell carcinomas and pancreatic adenocarcinomas) but has not been reported in meningiomas. On immunohistochemical study, the expression of p16 (*CDKN2A*) was absent or very weak in all the cases harboring the *CDKN2A* p.Ala148Thr mutation. However, the analysis of the whole series did not show any significant relation between p16 expression and tumor recurrence. Mean follow-up was 60±75 months and mean PFS 75±73 months. PFS was shorter in grade II and III vs. grade I meningiomas ($p=0.002$) and, in tumors with a mitotic index ≥ 4 ($p=0.03$) and a Ki67 index $> 5\%$ ($p=0.047$). Presence or absence of the *CDKN2A* p.Ala148Thr mutation had no influence on PFS.

Conclusions: Our study identified a novel mutation of *CDKN2A* potentially involved in meningiomas recurrence. However, the physiopathological role of this alteration remains to be clarified. In addition, it would be interesting to know whether this mutation is associated with other alterations of genes regulating the cell cycle and, if so, how they could cooperate.

1825 PREVIOUSLY PUBLISHED

1826 BRAF, NRAS and PIK3CA Mutations in Cases of Orbital Erdheim-Chester Disease

Khadijeh Jahanseir¹, James A Garrity¹, Benjamin Kipp¹, Diva Salomao¹. ¹Mayo Clinic, Rochester, MN

Background: Erdheim-Chester disease (ECD) is a type of Langerhans cell histiocytosis. Orbital involvement is rare and often challenging to diagnose and manage. Studies have shown 70-100% of cases harbor *BRAF V600E* mutation which can respond to vemurafenib. A recent study identified *PIK3CA* and *NRAS* mutations in a small subset of *BRAF V600E* mutant as well as wild-type ECD that might provide different targets for therapy, especially in *BRAF* wild-type cases.

Design: Institutional files (1990-2016) search identified 20 cases with diagnosis of orbital ECD, xanthogranulomatous infiltrate and xanthogranuloma. Cases were reviewed and diagnosis of ECD was made in 5 cases. Clinical information was collected. All cases were screened for *BRAF V600E* mutation by IHC. Next generation sequencing was performed to detect *BRAF*, *NRAS* and *PIK3CA* mutations.

Results: 3 M and 2 F with age ranging from 50-75 years (mean 61) were identified. Orbital presentation varied from diplopia/proptosis (n=1), tearing/eyelid swelling (n=1), fluctuating vision/eye irritation (n=1) or recurrent xanthelasma (n=1). One case had no ophthalmic symptoms and the bilateral masses were incidentally found on a brain MRI. On the imaging, all cases had bilateral intraocular orbital masses or infiltrates. Other organs involved were: perinephric soft tissue (3/5), paranasal sinus (3/5), brain (3/5), lung (2/5), peritoneum (1/5), bone (1/5). One case had diabetes insipidus. The follow-up duration ranged from 5-84 months (mean; 40.2). Two cases with molecularly confirmed *BRAF V600E* mutations were treated with vemurafenib. One had dramatic response resulting in no residual disease, the other stopped treatment due to severe drug reaction. Two cases received chemotherapy and immunosuppression. On the last follow up, 4 patients were alive with disease and 1 was alive without disease. All cases were positive for *BRAF V600E* on IHC. Two cases did not have sufficient DNA for sequencing. The 3 remaining cases had *BRAF V600E* mutation by sequencing, one harbored a *TET2* gene mutation and clinically had concomitant CMML. We did not identify mutations on *NRAS* or *PIK3CA* genes.

Conclusions: In our study, *BRAF V600E* mutation was identified in all cases by IHC and in 3 cases with sufficient DNA for genome sequencing. A complete response was achieved in the patient who received vemurafenib. *NRAS* and *PIK3CA* mutations were not detected in our cases. Albeit this is a small case series, the alternative mutations were only seen in a small subset of cases in prior studies.

1827 Expression of Renal Cell Markers and Detection of 3p Loss links Endolymphatic Sac Tumor to Renal Cell Carcinoma and Warrants Careful Evaluation to Avoid Diagnostic Pitfalls

Rachel L Jester¹, Iya Znoyko², Maria Garnovskaya², Tuan Tran³, Jason Mull⁴, Mary Richardson⁵, Dayna Wolff⁶, Adriana Olariu⁶. ¹Medical University of South Carolina, Charleston, SC, ²Medical University of South Carolina, ³Baylor University Medical Center, ⁴University of Texas Southwestern Medical Center, ⁵MUSC, Charleston, SC, ⁶Medical University of South Carolina, Charleston, SC

Background: Endolymphatic sac tumor (ELST) is an extremely rare neoplasm arising in the temporal petrous region thought to originate from endolymphatic sac epithelium and only recently recognized as a distinct entity. It may arise sporadically or in association with Von-Hippel-Lindau syndrome (VHL). The ELST prevalence in VHL ranges from 3-16% and may be the initial presentation of the disease. Onset is usually in the 3rd to 5th decade with hearing loss and an indolent course. ELSTs present as locally destructive lesions with characteristic CT imaging features and histology with papillary, cystic or glandular architectures. They immunohistochemically express keratin, EMA, and variably S-100, GFAP, and NSE. Currently it is recommended that given its rarity, ELST needs to be differentiated from other entities with similar morphohistologic patterns, including metastatic renal cell carcinoma (RCC).

Design: Four sporadic ELST cases were evaluated with immunohistochemistry and single nucleotide polymorphism microarray testing. Comparison with the RCC immunophenotype and copy number profiles was performed.

Results: Four adult patients presented with characteristic destructive lesions in the petrous temporal bones without clinical evidence of VHL including the presence of other VHL-related tumors (i.e. RCC, hemangioblastomas). Full *VHL* gene sequencing was previously performed in one patient with wild-type results. Pathology of tumors showed characteristic ELST morphology with immunohistochemical expression of CK7, GFAP, PAX-8, PAX-2, CA9 in the tumor cells. RCC marker, CD10, GATA3, CK20, S100, chromogranin, synaptophysin, SMA, TTF1, thyroglobulin, transthyretin were negative in the tumor cells. Preliminary molecular testing showed loss of 3p (including the *VHL* gene), 4q, and 9p.

Conclusions: Immunoreactivity for renal markers in ELST is an important diagnostic caveat and has not been previously reported. In fact, renal markers are currently recommended in order to rule out metastatic RCC; however, there is evidence to suggest that *PAX* gene complex and *CA9* have been implicated in the development of the inner ear. Importantly, genotyping of ELST has not been previously reported, and loss of 3p (which includes the *VHL* locus) in ELST suggests similar mechanistic origins as RCC. We are currently expanding our cohort of cases to confirm these novel findings.

1828 Transcriptomic Analysis Reveals Astroblastomas that Cluster with HGNET-BCOR not HGNET-MN1

Bette Kleinschmidt-DeMasters¹, Nicholas Willard², Andrew Donson³, Nicholas K Foreman⁴. ¹University of Colorado Anschutz Medical Campus, Aurora, CO, ²University of Colorado Anschutz Medical Campus, ³The Children's Hospital Colorado, ⁴Children's Hospital Colorado

Background: DNA methylation studies (Sturm *et al.*) have suggested that embryonal tumors of the central nervous system (CNS), formerly designated CNS-primitive neuroectodermal tumors (CNS-PNETs) cluster into 4 distinct groups: high grade glioneuronal tumors (HGNET)-BCOR, HGNET-MN1, NB-FOXR2, and EFT-CIC, with embryonal tumors with multilayered rosettes, now ETMR-C19 altered, occupying a distinct 5th group. Astroblastomas were found in the original study exclusively in the HGNET-MN1 group. RNA assessment by transcriptomic analysis (microarray gene chip) can also show this grouping and generally correlates well with histopathological diagnosis, as does DNA methylation. Within our dataset we hypothesized that cases from our files previously-diagnosed as astroblastoma would cluster as HGNET-MN1 and medulloepitheliomas/ embryonal tumor with abundant neuropil and true rosettes would cluster tightly as a distinct group.

Design: Affymetrix microarray transcriptomic data from file cases of histologically-diagnosed CNS-PNET, astroblastoma, or ETMR. Unsupervised hierarchical clustering analysis was performed using R bioinformatics.

Results: 22 pediatric tumors met inclusion criteria. Signature transcripts for each subgroup as identified by Sturm *et al* grouped 5 of 6 astroblastoma-histology tumors as HGNET-MN1. The 6th, however, was high grade, albeit histologically-classic, and developed metastases with 8 months; both original and metastatic samples closely clustered with HGNET-BCOR tumors in our dataset. All 6 ETMRs (all LIN28a IHC+) clustered tightly together; these tumors had original histological diagnoses of medulloepithelioma (n=1) or embryonal tumor with abundant neuropil and true rosettes (ETMR) (n=4), and thus, clustering was as expected. However, 1 of 6, even on histological review, remained a relatively patternless PNET-like small blue cell tumor without rosettes and was proven to be ETMR only by transcriptomic analysis + LIN28a IHC+. Samples that grouped into EFT-CIC (n=1), NB-FOXR2 (n=6), and HGNET-BCOR (n=3) were less distinctive histologically.

Conclusions: Transcriptomic analysis reveals occasional astroblastomas that cluster as HGNET-BCOR rather than HGNET-MN1.

1829 Clinicopathologic Features of Anaplastic Myxopapillary Ependymomas

Julieann Lee¹, Nima Sharifai², Sonika Dahiya³, Bette Kleinschmidt-DeMasters⁴, Marc Rosenblum⁵, Gerald Reis⁶, David Solomon¹, Tarik Tihan¹, Arie Perry¹. ¹University of California San Francisco, San Francisco, CA, ²Washington University in Saint Louis, ³Washington University in St. Louis, Saint Louis, MO, ⁴University of Colorado Anschutz Medical Campus, Aurora, CO, ⁵Memorial Sloan-Kettering CC, New York, NY, ⁶Memorial Regional Hospital, Hollywood, FL,

Background: Myxopapillary ependymomas (MPE) are considered benign (WHO grade I) neoplasms with a favorable prognosis. However, more aggressive biologic behavior, such as local recurrence, invasion, spinal metastases, and brain metastases may be seen. Only three cases of myxopapillary ependymomas demonstrating anaplastic features have been reported in the literature thus far, all occurring within the pediatric setting. The 2016 WHO describes anaplasia as most exceptional, and diagnostic criteria have not been defined.

Design: We encountered eleven cases of anaplastic myxopapillary ependymomas from five institutions. By definition, they included at least two anaplastic features: ≥ 5 mitoses per 10 high power fields, MIB-1 labeling index (LI) $\geq 10\%$, microvascular proliferation, or necrosis, typically in foci of hypercellularity and reduced mucin.

Results: There were 6 male and 5 female patients (age range 6-57 years; median 32 years). Seven displayed anaplasia at initial resection, while four became anaplastic at the time of recurrence, 9 months to 14 years subsequently. The maximal mitotic index ranged from 3 to 20 (median 7). The MIB-1 LI ranged from 8.5-40%, with the LI in foci of classic MPE typically being $<3\%$. There was CSF dissemination in 8/11 cases, documented recurrence after anaplasia in four cases, and invasion of adjacent bone/soft tissues in four cases. One case had metastatic disease to the lung.

Conclusions: Although rare, features of anaplasia can be found in both pediatric and adult MPEs, similar to other ependymomas. At a minimum, closer clinical observation is recommended, given the more aggressive biologic potential. Further study is needed to determine WHO grading implications.

1830 Identifying epithelial-mesenchymal transition (EMT) factor in relation with tumor progression and therapeutic resistance of malignant glioma

Jae-Hyuk Lee¹, Nah Ihm Kim², Kyung Hwa Lee³, Kyung-Sub Moon². ¹Chonnam National University Hwasun Hospital, Gwangju, ²Chonnam National University Hwasun Hospital, ³Chonnam National University Hwasun Hospital, Hwasun-gun, Jeollanam-do

Background: Glioblastoma is the most aggressive form of brain tumors, as they are growing fast and prone to infiltrate into the surrounding parenchyma. The current treatment is surgery to remove the tumor as much as possible, in combination with chemoradiation. Invasive phenotype and cancer stemness that promote resurgence of residual tumor cells is the major obstacle in glioblastoma treatment. Hence identifying primary factor of epithelial-mesenchymal transition (EMT) related with invasion and stemness of glioblastoma is critical in setting a therapeutic strategy.

Design: Hypermotile glioma cell lines were established through a repetitive scratch method using U87, U251, and U118 cell lines. Then altered tumor invasiveness and stemness were explored in vitro. Changes in expression levels of EMT and stemness factors were investigated by Western blot analysis and real-time polymerase chain reaction (PCR). Colony forming assay was performed in addition to invasion and migration assay. Selected EMT factor expression was examined in human glioma samples by immunohistochemistry and its effect on glioma patient survival rates was also analyzed.

Results: Established hypermotile glioma cell lines showed enhancement of invasion and migration capacity and also formed a

larger number of neurospheres than original glioma cells. Of EMT markers, SLUG has been consistently increased by Western blot analysis and real-time PCR. Up-regulation of SLUG expression resulted in increased invasion capacity and knockdown of SLUG expression was associated with decreased invasion. While overall survival rates were not significantly affected by SLUG expression levels, the group with low SLUG expression had longer progression-free survivals than the group with high SLUG expression (P=0.042). In addition, infiltrating single glioma cells frequently exhibited strong SLUG expression in the invasion front of human glioblastoma samples.

Conclusions: Through establishment of hypermotile glioma cell lines using a repetitive scratch method, SLUG was named as a promising candidate that is expected to play a pivotal role in glioma progression in terms of invasive phenotype and stemness. More biological roles of SLUG in relation with chemoradiation need to be elucidated to set a potential therapeutic target.

1831 Implementation of the 2016 WHO Classification for Infiltrating Glioma: The VGH Experience

Adrian B Levine, Stephen Yip. University of British Columbia, Vancouver, BC

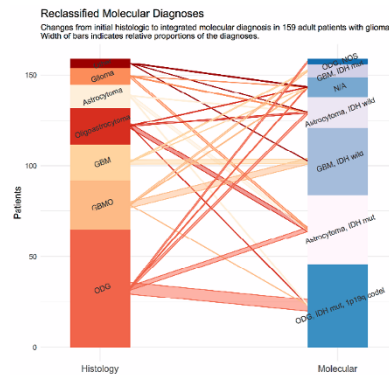
Background: The classification system for gliomas has undergone significant revisions in the last several years, with the incorporation of molecular criteria and removal of mixed histologic diagnoses. Large-scale molecular studies have elucidated the biological characteristics of low-grade gliomas, and enabled grouping based on isocitrate dehydrogenase (IDH) mutational and 1p19q codeletion status that outperforms histology in predicting patient outcomes. Mutations in *ATRX* and *TP53* are largely mutually exclusive with 1p19q codeletion in the context of mutant IDH, and are useful in screening patients for further molecular studies.

Design: Our study was conducted at a single institution with five staff neuropathologists. At our institution, new testing methods for 1p19q codeletion were implemented in 2014, and we have included all 159 cases submitted for 1p19q FISH testing since this time. Pathology reports were reviewed for histologic diagnoses, IDH R132H, *ATRX*, and P53 immunohistochemistry. Slides were reviewed for cases with unclear results and further testing ordered for a subset of cases. Histologic diagnoses were reclassified per 2016 criteria, incorporating molecular test results.

Results: We have found that retention of *ATRX* nuclear expression (indicating wild type *ATRX*), in patients with IDH mutation, is highly sensitive and specific for 1p19q codeletion. However the *ATRX* immunohistochemical test can be challenging to interpret and there have been a small number of discordant results. In comparing histologic to molecular diagnoses, the majority of histologic oligodendrogliomas indeed have 1p19q codeletion, while oligoastrocytomas and GBMOs largely show 1p19q retention of heterozygosity and are re-classified as astrocytomas and glioblastomas, respectively.

Predictive value of IDH and ATRX for 1p19q codeletion			
		1p19q	
		positive (codelet)	negative (retained)
IDH + ATRX	positive (IDH mut, ATRX wt)	39	10
	negative (other)	8*	77

*5 are IDH wt/ATRX wt, and 3 are IDH mut/ATRX mut



Conclusions: *ATRX* immunohistochemistry is a useful predictive test for 1p19q codeletional status, but should be interpreted in the context of histology and clinical features. Discordant results can arise both from technical issues of the test and the underlying biology of the tumor. With molecular testing, the majority of tumors with mixed histology were re-classified as astrocytic.

1832 The Genetic Landscape of Gliomas Arising After Therapeutic Radiation for Childhood Cancer

Giselle Lopez, Andrew Bollen, Tarik Tihan, Arie Perry, David Solomon. University of California, San Francisco, San Francisco, CA

Background: Although radiation therapy can be curative for pediatric cancers, secondary malignancy is a known complication. The genetic alterations underlying secondary gliomas arising after therapeutic radiation remain poorly characterized.

Design: Eleven gliomas arising after radiation treatment for childhood cancer were identified at our institution between 2008 and 2017, all of which were located within the radiation field. The cases were reviewed and studied by capture-based next-generation sequencing to assess approximately 500 cancer-associated genes for mutations, structural variants, and copy number alterations.

Results: The most common primary malignancies were medulloblastoma (n=4), leukemia (n=2), and germinoma (n=2). The average interval to glioma diagnosis was 15 years (range 4-40 years), including glioblastoma (n=5), anaplastic astrocytoma (n=4), pleomorphic xanthoastrocytoma (n=1), and low-grade glioneuronal neoplasm (n=1). All nine high-grade astrocytomas demonstrated markedly aneuploid genomes with several chromosomes per tumor demonstrating numerous segmental gains and losses consistent with "chromothripsis". Additional changes in these nine tumors included *TP53* mutation (n=6), *PDGFRA* amplification and/or mutation (n=6), *CDKN2A/B* homozygous deletion (n=4), and *CDK4* amplification (n=3). Three tumors harbored *BRAF* gene fusions or rearrangements, including the pleomorphic xanthoastrocytoma. The low-grade glioneuronal neoplasm demonstrated homozygous *SMARCB1* deletion only. None of the 11 tumors had *IDH1*, *IDH2*, *H3F3A*, *HIST1H3B*, or *TERT* promoter mutations.

Conclusions: The majority of gliomas arising after therapeutic radiation treatment are pathologically consistent with anaplastic astrocytoma or glioblastoma, which genetically differ, in part, from their spontaneous counterparts. They are characterized by marked aneuploidy, likely arising from the chromosomal breaks induced by gamma-irradiation. Furthermore, *TP53*, *PDGFRA*, *CDKN2A*, *CDK4*, and *BRAF* alterations are common. These findings identify a genetic signature of radiation-associated gliomas that is distinct from their spontaneous counterparts and suggest that different therapeutic strategies may be required for these secondary malignancies.

1833 Aberrant ATRX Protein Expression is Associated with Worse Survival in NF1-Associated Malignant Peripheral Nerve Sheath Tumors

Hsiang-Chih Lu¹, Anthony J Apicell², Vanessa Eulo², Melike Pekmezci³, Angela C Hirbe², Sonika Dahiya⁴. ¹Washington University School of Medicine, St Louis, MO, ²Washington University School of Medicine, ³Univ. of California, San Francisco, San Francisco, CA, ⁴Washington University in St. Louis, Saint Louis, MO

Background: Malignant Peripheral Nerve Sheath Tumors (MPNSTs) are soft tissue sarcomas that can arise either sporadically or in patients with Neurofibromatosis type 1 (NF1). Recently, *ATRX* mutations had been identified in a subset of MPNSTs. We further explored its role in a relatively large cohort of sporadic and NF1-associated MPNSTs, as well as plexiform neurofibromas.

Design: Immunohistochemistry for *ATRX* was performed on a retrospective cohort of MPNSTs and plexiform neurofibromas diagnosed at two institutions.

Results: MPNSTs were more likely to display aberrant *ATRX* expression pattern (mosaic or loss) compared to plexiform neurofibromas (53% vs. 6%, p<0.01). Furthermore, aberrant *ATRX* protein expression was associated with a significantly decreased overall survival in NF1-associated MPNSTs [median survival 14.5 months (aberrant *ATRX* expression) vs. >120 months (retained *ATRX* expression), p=0.01], while there was no difference in overall survival based on *ATRX* protein expression pattern for sporadic MPNSTs [median survival 80.7 months (aberrant *ATRX* expression) vs. 94.4 months (retained *ATRX* expression), p=0.81].

Conclusions: In contrast to plexiform neurofibromas, aberrant *ATRX* protein expression is seen in a large subset of MPNSTs. Of note, this aberrant *ATRX* protein expression is associated with decreased overall survival in NF1-associated MPNSTs, but not sporadic MPNSTs. These observations hint towards a potentially distinct biology of the nerve sheath tumors in the two groups, and beg further investigation.

1834 What Key Features Should Prompt Evaluation for Atypical Pituitary Adenoma by p53 and Ki67 Immunostaining?

Laura Malone¹, Rachel E White², Cheng-Ying Ho¹. ¹University of Maryland Medical Center, Baltimore, MD, ²University of Maryland, Baltimore, MD

Background: Atypical pituitary adenomas are defined by World

Health Organization classification as tumors with increased mitotic activity, excessive p53 staining, and a Ki67 proliferation index of at least 3%. Clinically, atypical adenomas exhibit more aggressive growth and require close monitoring. As only 5% of pituitary adenomas are atypical, performing p53 and Ki67 staining on all cases is likely neither practical nor necessary. Therefore, we aim to identify key clinical, radiologic, or histologic characteristics that can be used to prompt further evaluation by p53 and Ki67 immunostaining.

Design: Sixteen cases of atypical pituitary adenomas (M:F = 12:4, age 15-74) and 20 randomly selected cases of non-atypical pituitary adenomas (M:F = 12:8, age 24-79) were collected from our institution. Demographic information, tumor size, functional status, hormonal positivity by immunohistochemical (IHC) staining, and mitotic rate were compared between the two groups.

Results: The mean age at diagnosis of patients with atypical adenomas was 39.5 versus 49 for patients with non-atypical adenomas (Student's t-test, p value = 0.039). 50% of atypical adenoma patients were less than 40 years compared to 15% of non-atypical adenoma patients (chi-square test, p value = 0.023). 77% of atypical pituitary adenomas measured greater than 3 cm compared to 31% of non-atypical adenomas (chi-square test, p value = 0.036). Lastly, 56% of atypical adenomas were found to be IHC hormone positive compared to 20% of non-atypical adenomas (chi-square test, p value = 0.024). The differences in patients' gender, functional status of the tumors, and rare mitotic figures are not statistically significant.

	Atypical pituitary adenomas	Non-atypical pituitary adenomas	P-value *statistically significant
Age			
Median age	39.5 yo	49 yo	0.039*
<30yo	25% (4/16)	5% (1/20)	0.085
<35yo	37.5% (6/16)	10% (2/20)	0.049*
<40yo	50% (8/16)	15% (3/20)	0.023*
<45yo	62.5% (10/16)	35% (7/20)	0.101
<50yo	62.5% (10/16)	50% (10/20)	0.453
Gender			
Male	75% (12/16)	60% (12/20)	0.343
Female	25% (4/16)	40% (8/20)	0.343
Functional	15% (4/16)	10% (2/20)	0.230
ACTH	6.25% (1/16)	5% (1/20)	
GH	18.75% (3/16)	0% (0/20)	
Prolactin	0% (0/16)	5% (1/20)	
Size			
Median size	3.3 cm	2.7 cm	0.433
>2.5cm	80% (16/20)	63.63% (14/22)	0.241
>3cm	75% (15/20)	36.36% (8/22)	0.012*
>3.5cm	45% (9/20)	18.18% (4/22)	0.060
>4cm	40% (8/20)	13.63% (3/22)	0.052
>4.5cm	15% (3/20)	9.09% (2/22)	0.555
IHC hormone positivity	68.75% (11/16)	35% (7/20)	0.044*
ACTH	12.5% (2/16)	5% (1/20)	0.418
FSH	12.5% (2/16)	15% (3/20)	0.829
LH	0% (0/16)	10% (2/20)	
GH	25% (4/16)	5% (1/20)	0.085
Prolactin	37.5% (6/16)	15% (3/20)	0.121
Median mitotic rate	2.5 mits / 10 HPF	0 mits / 10 HPF	0.00009*
HPF)			
No increase	12.5 % (2/16)	82.35% (14/17)	0.00006*
(0 per 10			
Rare	6.25% (1/16)	11.76% (2/17)	0.582
(1 per 10			
Mild	25% (4/16)	5.88% (1/17)	0.126
increase			
(2 per 10			
HPF)			

Conclusions: Our study indicates that pituitary adenomas occurring in individuals younger than 40 years old, measuring greater than 3cm, and showing IHC hormone positivity are statistically more likely to be atypical adenomas and will require further evaluation by p53 and Ki67 IHC staining.

1835 VEGF-121 plasma level as biomarker for response to anti-angiogenetic therapy in recurrent glioblastoma

Maurizio Martini¹, Quintino Giorgio D'Alessandris², Ivana De Pascalis³, Lucia Ricci-Vitiani⁴, Francesco Pierconti⁴, Vincenzo Fiorentino⁵, Roberto Pallini⁶, Luigi Maria Larocca⁷. ¹Catholic University of Sacred Heart, Roma, ²Catholic University of Sacred Heart, Rome, ³Istituto Superiore di Sanità, Rome, Italy, ⁴Catholic University of Sacred Heart, Roma, Italy, ⁵Catholic University of Sacred Heart, Roma, Italia, ⁶Catholic University of Sacred Heart, Rome, Italy, ⁷Fondazione Policlinico Universitario A. Gemelli, Rome, Italy

Background: Glioblastoma (GB) is one of the most vascularized human tumors. We have recently shown that GB is able to produce all vascular endothelial growth factor (VEGF) isoforms and that its sensitivity to anti-angiogenetic therapy may depend on the relative amount of the various isoforms. The diffusible VEGF-121 isoform could play a major role in the response of recurrent glioblastoma to treatment with bevacizumab. We hypothesized that circulating VEGF-121 may reduce the amount of bevacizumab available to target the heavier isoforms of VEGF, which are the most clinically and biologically relevant.

Design: We assessed the plasma level of VEGF-121 in a brain xenograft model, in human healthy controls, and in patients suffering from recurrent GB before and after bevacizumab treatment. We also evaluated the relationship between the VEGF-121 plasma level and the tumor size in xenograft and contrast enhancing tumor (CE) area in patients. Data was matched with patients' clinical outcome.

Results: In athymic rats with U87MG brain xenografts, the level of plasma VEGF-121 relates with tumor volume and it significantly decreases after intravenous infusion of bevacizumab. Patients with recurrent GB show higher plasma VEGF-121 than healthy controls ($p=0.0002$) and treatment with bevacizumab remarkably reduced the expression of VEGF-121 in plasma of these patients ($p=0.0002$). Interestingly the VEGF-121 plasma level directly correlated with the VEGF-121 mRNA in the tumor and with CE area at the MRI. Higher plasma level of VEGF-121 and higher Δ VEGF-121 (VEGF-121 pre bevacizumab infusion - VEGF-121 after bevacizumab infusion) predict worse PFS and OS ($p=0.0001$ and $p=0.0003$, and $p=0.0013$ and $p=0.0008$, respectively).

Conclusions: VEGF-121 plasma level in the recurrent GB reflect the size and the angiogenetic process in the tumor. Quantitative analysis of VEGF-121 isoform plasma level is a biomarker for patients with recurrent GB tumors, predicting the response to anti-angiogenetic treatment.

1836 MUC4 expression in meningiomas: Under-recognized immunophenotype particularly in meningeothelial/epithelioid cells

Atsuji Matsuyama¹, Eisuke Shiba², Masanori Hisaoka³. ¹University of Occupational & Environmental Health, Kitakyushu, Japan, ²University of Occupational and Environmental Health, ³Univ of Occupational & Environ, Kitakyushu, Fukuoka, Japan

Background: MUC4 is a high molecular weight transmembranous glycoprotein that plays a role in a cell growth signaling pathway and expressed in various epithelia to serve protective roles. The gene expression profiling assay and the immunohistochemical analyses revealed that MUC4 is also constantly and specifically expressed in low grade fibromyxoid sarcomas and sclerosing epithelioid fibrosarcomas among the mesenchymal tumors and its immunohistochemical detection is extremely useful for their diagnoses. Incidentally, we noticed that meningiomas are often positive for MUC4 in our routine pathological practice and this finding still remains poorly investigated, despite the extensive scrutiny of its expression in soft tissue tumors.

Design: We immunohistochemically examined the expression of MUC4 in 43 meningiomas of variable histological subtypes, including 5 extracranial tumors (2 in spinal cord, 2 in middle ear, 1 in paranasal sinus). Ten intracranial schwannomas, 4 meningeal solitary fibrous tumors, 6 hemangioblastomas and 2 sinonasal glomangiopericytomas were also tested.

Results: In the 43 meningiomas, 40 (93%) expressed MUC4, at least focally (6/9 in fibrous, 8/8 in meningeothelial, 4/4 in angiomatous, 1/1 in secretory, 7/7 in other grade 1 subtypes, 1/1 in clear cell, 8/8 in atypical, 5/6 in anaplastic). MUC4 expression was much more common in meningeothelial or epithelioid cells than spindle or fibrous cells. The positive tumor cells were only scattered and limited in <5% of tumor cells in 5 tumors, but other tumors showed the diffuse or localized expression (median, 40% of tumor cells). Among the tumors with limited expression or negativity of MUC4, 6 were fibrous subtype, 1 each was psammomatous, atypical and anaplastic. All the schwannomas, solitary fibrous tumors, hemangioblastomas and sinonasal glomangiopericytomas examined were negative for MUC4.

Conclusions: MUC4 is variably, but almost constantly expressed in meningiomas, particularly in cells with meningeothelial/epithelioid features. Its immunohistochemical detection may be useful to distinguish meningiomas from other meningeal or head and neck mesenchymal tumors, particularly those with epithelioid features. Our study could expand a variety of MUC4-positive mesenchymal tumors.

1837 Molecular Characterization of Pediatric Supra-Tentorial Diffuse Gliomas: Identification of Mutational and Prognostic Subgroups

Sarah Meunier¹, Blandine Boisselier¹, Emilie De Carl², Philippe Mene¹, Philippe Guardiola¹, Audrey Rousseau². ¹Angers University Hospital, ²Angers University Hospital, Angers, Maine et Loire, ³Angers

Background: Pediatric (PD) supra-tentorial diffuse gliomas are rare central nervous system tumors. PD patients are usually treated according to adult therapeutic regimens even though PD gliomas develop along distinct genetic pathways compared to their adult counterparts. The main objective of this work was to study PD supra-tentorial diffuse gliomas diagnosed at our institution, to identify distinct mutational and prognostic subgroups.

Design: Thirty eight cases were studied by immunohistochemistry (antibodies against H3K27me3, IDH1-R132H, ATRX, p53, BRAF-V600E, MSH6, PMS2, MLH1, MSH2). Sanger sequencing of IDH1/2, HIST1H3B, H3F3A, BRAF and FGFR1 genes and pangenomic SNP arrays were performed. Clinical, radiological and survival data were obtained for each patient.

Results: Four mutational subgroups were identified, associated with significantly different overall survival, location (hemispheric vs midline) and age at diagnosis ($p=0.007$, 0.001 , 0.002 , respectively). The subgroup "H3K27M mutant gliomas" (31% cases), defined by a H3K27M mutation, was comprised of midline tumors (100%) in children (median age 11.3 years) with a poor outcome (median overall survival 8.6 months). The subgroup "H3G34R mutant gliomas" (8% cases), defined by a H3G34R mutation, was comprised of hemispheric tumors with ATRX mutation (100%) in teenagers (median age 15.2 years). Prognosis seemed better compared to that of H3K27M mutant gliomas. The subgroup "IDH mutant gliomas" (16% cases), defined by an IDH mutation, was comprised of hemispheric tumors arising in young adults (median age 23.5 years) with ATRX mutation and no 1p/19q codeletion (diffuse astrocytomas) and the longest survival. The last subgroup "wild-type (WT) gliomas", WT for IDH1/2, H3.3/H3.1, BRAF and FGFR1 genes, comprised 45% of the cases. These tumors, mostly hemispheric, affected younger children (median age 8.9 years) with a median survival time of 22.7 months. No constitutional mismatch repair deficiency syndrome was detected in the WT subgroup.

Conclusions: We have identified 4 mutational subgroups (H3K27M, H3G34, IDH and WT) significantly associated with distinct age, tumor location and prognosis. Driver genes are yet to identify in WT gliomas; such an identification will require high throughput sequencing techniques. Molecular classification of PD supra-tentorial diffuse gliomas is an essential step in the management of the patients and should allow personalized therapeutic approaches in the near future.

1838 Questionable role of ZEB1 in malignant gliomas: Altered expression of ZEB1 correlates with invasiveness in glioma cell-lines, not with clinical prognosis

Kyung-Sub Moon¹, Nah Ihm Kim¹, Jae-Hyuk Lee², Kyung Hwa Lee³. ¹Chonnam National University Hwasun Hospital, ²Chonnam National University Hwasun Hospital, Gwangju, Gwangju, ³Chonnam National University Hwasun Hospital, Hwasun-gun, Jeollanam-do

Background: Although ZEB1, a key inducer of epithelial mesenchymal transition (EMT), has been reported to promote tumor invasion and metastasis in various cancers, the role of ZEB1 in malignant gliomas has not been fully investigated. The aim of this study was to investigate the effect of ZEB1 on biological behaviors in human gliomas cell lines and on patient survival data.

Design: To evaluate the role of ZEB1 in glioma invasiveness, cell invasion and migration capabilities were investigated after ZEB1 knockdown using small-interfering RNA. ZEB1 expression was examined in 89 human glioma samples by immunohistochemistry. Comparison of ZEB1 expression in each histological grade, and its effect on glioma patient survival rates were also analyzed.

Results: ZEB1 knockdown resulted in significantly reduced cell invasion and migration in U251 and T98G cell lines. ZEB1 down-regulation also caused diminished expression of EMT related factors and genes by Western blotting and RT-PCR. ZEB1 expression, however, did not correlate with WHO tumor grades, overall survival rates, and progression free survival. Kaplan-Meier analysis did not reveal statistically significant difference of survival period between the high ZEB1 expression group and the low expression group in our patient cohort as well as in the large data set, Repository for Molecular Brain Neoplasia Data (REMBRANDT) by National Cancer Institute (NCI).

Conclusions: ZEB1 knockdown lead to decreased invasiveness and migration with reduced expression of EMT related factors and genes in glioma cell lines. However, ZEB1 expression in human glioma sample did not reveal a notable correlation with patient survival rates or clinicopathological variables.

1839 Whole Exome and Targeted Sequencing of Adult Infiltrating Astrocytomas: Experience at a Single Institution

Samaneh Motanagh¹, Andrea Sboner², Kenneth Eng³, Michael Kluk⁴, Juan Miguel Mosquera⁴, Howard A Fine², Mark Rubin⁴, Himisha Beltran⁵, Olivier Element⁵, Rohan Ramakrishna⁴, David Pisapia⁵. ¹Weill Cornell Medicine, New York, NY, ²Weill Cornell Medicine, ³Englander Institute for Precision Medicine, New York, NY, ⁴Weill Cornell Medical College, New York, NY, ⁵New York, NY

Background: Infiltrating astrocytomas (IA) comprise the most common primary brain tumors in the adult and include diffuse astrocytoma, WHO grade II (DA); anaplastic astrocytoma, WHO grade III (AA); and GBM (WHO grade IV). Histologically-based diagnoses belie a molecular heterogeneity within this spectrum of tumors that can be revealed by molecular methods such as whole exome sequencing as well as more targeted cancer panels. Herein we summarize our findings in an adult IA cohort enrolled as part of a precision medicine-based clinical trial at a single institution.

Design: We interrogated 85 IA samples over 81 distinct adults (4 DA, 20 AA, and 61 GBM), including 12 IDH-mutated astrocytomas. Whole exome sequencing was performed on fresh frozen or FFPE tumor tissue and matched peripheral blood samples for germline analysis; RNA-seq was done in a subset of samples. We present a summary of our findings as well as a comparison to more targeted approaches, such as the FoundationOne® sequencing panel (FO) available in 68 (80%) of cases, in order to assess distinct approaches to the molecular characterization of IA.

Results: The most frequently altered genes detected by both WES and FO include EGFR, CDKN2A/B, TP53, PTEN, NF1, IDH1, ATRX, and PIK3CA. Certain alterations such as TERT promoter mutations, which were present in the majority of IDH-wildtype IA's as detected by FO, were not assessed by WES. Several mutations in cancer related genes were revealed to be germline alterations in the WES pipeline alone, including in ARID1A, BRCA1, NF1, and WT1.

Conclusions: The majority of the most common recurrent genetic alterations in the spectrum of IA are reliably detected by WES and at comparable rates to more targeted panels such as FO; however exome sequencing pipelines should be tailored to additionally cover highly recurrent somatic alterations occurring within introns and promoters, such as TERT, and would benefit by higher coverage of critical regions. Germline assessment is important both for the interpretation of alterations detected in tumor tissue as well as for the overall management of the patient who may be at risk for multiple neoplastic processes.

1840 Does Post-Mortem Pituitary Histopathology Correlate with the BMI?

Behtash G Nezami¹, Mark Cohen², Bartolome Burguera³, Marta Couce⁴. ¹University Hospitals, Cleveland Medical Center, Beachwood, OH, ²University Hospitals Case Medical Center, Highland Heights, OH, ³Endocrinology and Metabolism Institute, Cleveland Clinic, Cleveland, OH, ⁴Bariatric and Metabolic Institute, Cleveland Clinic, Cleveland, OH, ⁴Cleveland, OH

Background: The link between chronic systemic inflammation and obesity has been well established, and may operate via stimulation of the hypothalamic pituitary axis by pro-inflammatory cytokines. Elevated plasma ACTH levels have also been correlated with excessive body weight. Additionally, little is known about the incidence of hypophysitis in the general population or its prevalence in obesity. Similarly, the incidence of ACTH hyperplasia/adenoma in obesity has also never been systematically studied. We therefore investigated the prevalence of hypophysitis and adeno/hypophysial hyperplasia/adenoma in our autopsy population in order to determine whether either of these histopathological abnormalities were overrepresented in patients with obesity.

Design: We retrospectively reviewed the histopathology of seventy two pituitaries removed from adult subjects at the time of autopsy between 2010 and 2017 at UHCMC. Cases with inflammatory CNS diseases were excluded (11 cases). The clinical history, body mass index (BMI) and cause of death were recorded. H&E, reticulin and IHC stains for ACTH, CD3 and CD20 were reviewed by two pathologists. Fisher and Chi square statistical tests were used.

Results: The patients were divided into 2 groups based on BMI: non-obese (BMI <30, N=29) and Obese (BMI ≥30, N=32), with mean ages of 59 and 57 years, respectively. The main cause of death was cardiac in both groups. Concomitant malignancies (predominantly pulmonary) were slightly more common in the non-obese group. Microscopic foci of inflammation were identified in 9 non-obese and 1 obese,

(39.1% vs. 10.0%, respectively, P=0.12) consisting predominantly of T lymphocytes at the adeno-neurohypophysial junction. Pituitary hyperplasia/adenoma, non-corticotroph, was identified in 6 obese and 1 non-obese subject (18.7% vs 3.4%, respectively, P=0.1). Variable amounts of adeno/hypophysial fibrosis was seen in 10 obese and 8 non-obese subjects.

Conclusions: Obese and non-obese patients demonstrated no significant differences in ACTH related pituitary pathology, possibly related to our limited sample size. However, non-corticotroph related pituitary hyperplasia/adenoma was identified more frequently in obese patients, whereas hypophysitis was more common in the non-obese group. Additional investigations are underway to correlate these findings with pre-mortem clinical differences in these patient populations. In addition, we are further characterizing the pituitary hyperplasias/adenomas within our autopsy population.

1841 NeuN Expression in Common Central and Peripheral Nervous System Tumors

Aivi Nguyen¹, Daniel Martinez², Bruce Pawel³, Paul J Zhang⁴. ¹Philadelphia, PA, ²Children's Hospital of Philadelphia, ³The Children's Hospital of Philadelphia, Cherry Hill, NJ, ⁴Hospital of the University of Pennsylvania, Media, PA

Background: NeuN is a neuron specific protein, seen in postmitotic neurons and differentiated cells of neurogenic tumors. The monoclonal antibody against NeuN stains neuronal nuclei and perikarya and is used in a variety of ontological and pathological assessments. However, a comprehensive and robust evaluation of common central and peripheral nervous system tumors has not yet been performed. This study aims to characterize NeuN expression in common pediatric and adult central and peripheral nervous system tumors.

Design: Immunohistochemistry for NeuN was performed on tissue microarrays (TMAs) procured from the Children's Hospital of Philadelphia Tissue Bank and individual surgical pathology cases from the Hospital of the University of Pennsylvania. The TMA cases included the following: 2 germinomas, 6 dysembryoblastic neuroepithelial tumors (DNETs), 19 medulloblastomas, 7 gangliogliomas, 2 neurocytomas, 13 cerebellar pilocytic astrocytomas, 7 supratentorial pilocytic astrocytomas, 167 neuroblastomas, 15 ganglioneuroblastomas, and 11 ganglioneuromas. Separate surgical pathology cases included 4 nonneoplastic dorsal root and sympathetic ganglion, 8 neuroendocrine tumors, 4 ganglioneuromas of the retroperitoneum or posterior mediastinum, and 8 gastrointestinal (GI) tract ganglioneuromas. Nuclear and perikaryon NeuN staining were considered positive. Blinded evaluation of TMA and surgical cases were performed independently by two reviewers.

Results: NeuN positivity was seen in neuronal components of DNETs and gangliogliomas, and tumor cells in medulloblastomas (Table 1). NeuN was negative in other neuronal neoplasms such as ganglioneuromas, ganglioneuroblastomas and pure glial tumors, CNS germ cell tumors and peripheral neuroendocrine tumors.

NeuN Positivity	
Histologic Diagnosis	NeuN Positivity
DNET	7/10
Ganglioglioma	4/7
Medulloblastoma	4/19
Neuroblastoma	1/167
Neurocytoma	1/2
Nonneoplastic ganglion	4/4
GI Ganglioneuroma	8/8

Conclusions: NeuN was a good marker for normal ganglion cells and was differentially expressed across pediatric and adult central and peripheral nervous system tumors, hinting at ontologic differences. It was not a generic marker for neuroendocrine tumors. NeuN was rarely expressed in neuroblastoma and downregulated in more matured neoplastic neuronal cells in ganglioneuroma and ganglioneuroblastoma. The diagnosis of ganglioneuromas vs nerve sheath tumor entrapping ganglions is often a diagnostic challenge, and NeuN positivity may aid in differentiating neoplastic ganglion versus entrapped normal ganglion. Lastly the finding of retained NeuN expression in GI mucosal ganglioneuroma prompts one to question if the ganglion cells are truly neoplastic in these lesions.

1842 Astrocytic tau deposition is frequent in Alzheimer disease and does not correlate with an atypical clinical presentation

Amber Nolan, Elisa De Paula Franca Resende, Cathrine Petersen, Alexander Ehrenberg, Salvatore Spina, William Seeley, Lea T Grinberg. University of California San Francisco, San Francisco, CA

Background: An important subset of patients with Alzheimer's disease (AD) present with atypical non-amnesic syndromes not explained by current staging schemes. Astrocytic tau accumulation increases with age but has yet to be well-characterized in relation to AD pathology and clinical presentation. Prior reports have linked tau-positive astrocyte clusters in the white matter with a primary progressive aphasia phenotype in AD. We hypothesized that co-existing astrocytic tau inclusions may change vulnerability of cortical networks and explain clinical heterogeneity.

Design: We systematically mapped astrocytic tau inclusions throughout selected cortical and subcortical sections in an AD cohort (N=76) enriched for atypical syndromes.

Results: Astrocytic tau accumulation was seen in 67% of cases overall and often clustered in distinct anatomical regions. Using principal component analysis, we identified co-existence in frontal (aCC, MFG, IFG) as well as limbic areas (ITG, insular, entorhinal cortices). Logistic regression revealed no relationship between presence of astrocytic pathology and atypical presentation. However, we observed an increase in astrocytic pathology with age. When examining morphological subtypes, thorn-shaped astrocytes (TSAs) in the white matter were associated with history of traumatic brain injury (TBI), and the aCC demonstrated a higher density of TSAs with prior TBI ($p < 0.05$). In depth analysis of the frontal and insular cortices revealed no significant role for astrocytic tau in producing bvFTD versus other AD syndromes; additionally, no correlation of executive function with astrocytic pathology was identified.

Conclusions: This study, the largest undertaken to date, does not support an association between astrocytic tau and AD clinical heterogeneity.

1843 Categorizing Peripheral Neuropathy Utilizing Deep Learning

Nkechi Okonkwo¹, Simukayi Mutasa², Cheng-Ying Ho¹. ¹University of Maryland Medical Center, Baltimore, MD, ²Columbia University Medical Center, New York, NY

Background: Morphometry allows for basic descriptions in quantitative terms and reveals minimal morphological differences between functional states. Clinically, morphometry has been used for objective diagnoses of peripheral neuropathies. Nerve morphometry evaluates individual nerve fibers manually, semi-automatically, or fully automated. Evaluation commonly includes number of axons, myelin sheath thickness, and the ratio of large vs. small-diameter axons. Because of the routine features used to categorize neuropathies, fully automated image analysis systems could be programmed to analyze nerve fibers but has not been well described. The aim of this study is to train a convolutional neural network (CNN) to recognize several pathological patterns of neuropathy.

Design: Toluidin-blue stained semithin sections from 23 peripheral nerve biopsy specimens were collected, including unremarkable biopsies and diabetic and vasculitic neuropathies. The data set consisted of high resolution nerve photomicrographs in transverse section. Hundreds of unique input images were generated from each image and fed into the network. Data augmentation was employed to improve generalizability performance of the network. 6 patients were sorted into the testing set and the rest were part of the training set.

A 13-hidden layer neural network was designed for the study. Hidden layers consisted of 12 residual and/or inception style layers with one fully connected layer and a three class softmax output. AUC was utilized as the primary performance metric. Accuracy, sensitivity and specificity were also calculated as secondary performance metrics. The network was trained using stochastic gradient descent with momentum. Due to the small patient size, statistical accuracy was evaluated by correct classification of each individual image patch for the unique patients in the testing set.

Results: Recognition of normal vs. abnormal had an accuracy of 86.5%, sensitivity of 71.0% and specificity of 99.5%. Overall macro AUC was 0.82. Accuracy was 75.5%, sensitivity was 0.63 and specificity was 0.92.

Conclusions: In this proof of concept study with 23 patients, we demonstrate that CNN's can be used to assist pathologists in diagnosing diabetic and vasculitic neuropathies, and possibly other types of neuropathies. This technique, can be used in peripheral nerves with the advantage of being a less expensive, more efficient method for diagnosing neuropathies. Further development with a larger data set can be employed to improve performance.

1844 Mutational Landscape and Risk of Tumor Recurrence in Meningioma

Adriana Olari¹, W Bailey Glen Jr.², Qianghu Wang³, Erik Sulman⁴, Kenneth D Aldape⁵. ¹Medical University of South Carolina, Charleston, SC, ²Medical University of South Carolina, ³University of Texas M.D. Anderson Cancer Center, ⁴MD Anderson Cancer Center UT Graduate School of Biomedical Science, ⁵Princess Margaret Cancer

CentreMacFeeters-Hamilton Brain Tumour Centre

Background: Meningioma carries a substantial risk of local recurrence. Although somatic mutational profiles of meningioma have been described their clinical implications are not well characterized. We hypothesized that meningiomas with unique mutational profiles could be used to better stratify patient management.

Design: Tumor samples (n=139) were profiled using next-generation sequencing methodology using a custom capture probe library for 36 genes. Variants were classified against publically available databases and based on allelic frequencies. Results were correlated with available whole-genome methylation and copy number profiles.

Results: The most common variants were in *NF2* [67/244, 27% in 67 patients (45%)] of which 32 (48%) were associated with chromosome 22 loss. The most common somatic variants involved *TRAF7* (13/95, 14%), *AKT1/KLF4/PIK3CA* (5/95, 5%), *SMO* (4/95, 4%), *TERT* promoter/*SMARCB1* (3/95, 3%), *RIMS2* (2/95, 2%), and *PTEN/SUFU/CDKN2C/RGPD3/CREBBP/EPB41L3* (1/95, 1%). In 12/13 (92%) *TRAF7* associated *AKT1/KLF4/PIK3CA* mutations as previously described but also *RGPD3* and *RIMS2* mutations. *NF2* mutations associated *TERT* promoter/*TRAF7/PTEN/SMARCB1/SUFU/CDKN2C/RIMS2/CREBBP/EPB41L3* mutations but were mutually exclusive with *PIK3CA/SMARCB1/ACT1/KLF4/SMO* mutations. All *PIK3CA/TERT* promoter/*KLF4/PTEN/SUFU* and most *NF2* (38/67, 57%), *TRAF7* (9/13, 69%), *SMO* (3/4, 75%), *EPB41L3* (6/7, 86%) mutations associated with a previously described prognostically unfavorable methylation subgroup associated with an increased risk for meningioma recurrence. On survival analyses the presence of *TERT* promoter and *PTEN* somatic mutations, *NF2*, *CDKN2C*, and *EPB41L3* variants were predictive of decreased recurrence-free survival (RFS) (log-rank $p < 0.0001$; $p = 0.0275$; $p = 0.0386$; $p = 0.0325$; $p = 0.0349$); however only the presence of *NF2* mutations remained associated with decreased RFS after adjusting for methylation subgroups, mitotic index, WHO/Simpson grades, sex, and copy number profiles ($p = 0.003$; Hazard ratio=3.06; 95%CI=1.16-11.59). All *SMARCB1/RGPD3/CREBBP/RIMS2* mutations associated with a previously described prognostically favorable methylation subgroup associated with a decreased risk for meningioma recurrence.

Conclusions: The presence of *NF2* mutations in meningioma patients is strongly associated with decreased RFS. Along with the WHO grade, mitotic index, methylation and copy number profiles, the *NF2* mutation status could be used to better stratify the risk for tumor recurrence and potentially guide patient management.

1845 Capture-Based 1,200 Gene Next-Generation Sequencing (NGS) Panel as a Comprehensive Tool for Classifying Gliomas According to the 2016 WHO System and for Characterizing Outlier Cases

Megan M Parilla, John Collins, Sabah Kadri, Sushant A Patil, Jeremy Segal, Carrie Fitzpatrick, Peter Pytel¹. University of Chicago, Chicago, IL

Background: The 2016 WHO classification of brain tumors represents a major step towards the integration of molecular data into pathologic diagnoses. Our institution has included a large NGS panel into the diagnostic work-up of gliomas in since 1/2016. The utilized platform successfully identifies copy number variations as well as mutations.

Design: The study was a retrospective review of data obtained from 51 glial tumor samples that had been run for clinical purposes using the OncoPlus platform, a 1,213 gene targeted hybrid capture NGS panel [see Kadri et al.; 2017 for details]. The DNA was prepared from FFPE tissue. Variant and copy number calling was performed using custom-designed computational pipelines.

Results: The NGS data allowed a reliable classification of the analyzed gliomas. The typical molecular profile of oligodendrogliomas (1p/19q co-deletion, IDH mutation, TERT promoter mutation) and K27M mutant midline gliomas were confirmed in all cases. Astrocytomas (grades II and III) and glioblastomas could be broken down into three categories based on their molecular profile: (1) IDH mutant cases, (2) IDH wild-type astrocytomas and glioblastomas with a molecular profile that included a TERT promoter mutation as well as at least one of the following: combined chr. 7 gain and chr. 10 loss, EGFR mutation/amplification, or CDKN2A loss. 77% of IDH wild-type tumors fell into this category. The astrocytomas in this group were confirmed to lack glioblastoma type imaging features at the time of surgery but exhibited aggressive growth akin to glioblastomas and may represent IDH wild-type glioblastomas diagnosed early. (3) The remaining IDH wild-type tumors, without the above molecular alterations, were a diverse group with heterogeneous biology. This group included tumors with unique molecular features, for example, a glioblastoma with DNMT3B mutation as well as an anaplastic astrocytoma with BRAF L485F mutation and CDKN2A loss. The clinical behavior of the tumors in this third group is arguably difficult to predict based on current data.

Conclusions: The full integration of a large NGS panel provides all information required for the classification of gliomas according to the 2016 WHO system in a single assay. It identifies copy number variations including 1p/19q status and mutations. Beyond that it

identifies potentially targetable alterations and helps to define those outlier cases that exhibit a more unusual molecular profile for which we cannot yet reliably predict behavior or treatment response.

1846 Genomic profiling of primary brain tumors: the UC San Diego Experience

Charmi Patel, Christina Di Loreto, Sarah Murray, Marie Dell'Aquila, Lawrence A Hansen, John Thorson. University of California San Diego, San Diego, CA

Background: Brain tumors have historically been classified according to histopathological criteria using microscopic examination of tissue sections. The World Health Organization (WHO) classification of central nervous system (CNS) tumors was revised in 2016, with integration of molecular parameters for the first time. In keeping with this change, the Neuropathology Division at our institution routinely obtains genomic profiling of all primary brain tumors and incorporates the results into the final pathologic diagnosis.

Design: Between September 2013 and July 2017, we performed genomic profiling consisting of next generation sequencing (NGS) using either a 47 gene panel or a 397 gene panel and genome-wide microarray analysis on 280 primary brain tumor specimens. Based upon initial histological diagnosis, the cohort included glioblastomas (40%), astrocytomas (16%) meningiomas (11%), and oligodendrogliomas (9%) as well as small numbers of ependymomas, pilocytic astrocytomas, and schwannomas. Nine percent of the specimens were initially assigned the non-specific diagnosis of glioma. NGS data were analyzed and variants were assigned to one of three significance categories: clinically significant, variant of uncertain significance, or not reportable. Microarray data was used to identify genomic structural changes, including segmental gains, losses, focal gene amplifications, and copy-neutral events such as loss of heterozygosity.

Results: One or more reportable genomic alterations were detected by NGS in 71% of cases. The most commonly mutated genes were *TP53* (39.4 % of cases), *IDH1* (31.3%), *PTEN* (14.6%), *PIK3CA* (9.1%), *EGFR* (8.6%) and *ATRX* (8.1%). Reportable cytogenetic abnormalities were detected in 95% of cases, including chromosome 7 gains, chromosome 9, 10, or 22 loss, and co-deletion of chromosomes 1p/19q. Clinically significant variants (those of diagnostic value or targetable with therapeutics) were identified in 75% of cases overall. For the majority of cases, molecular categorization was consistent with the initial histologic diagnosis. In addition, for a subgroup of cases which were histologically ambiguous or especially challenging, the genomic profiling information allowed provision of a clear or refined diagnosis.

Conclusions: This study demonstrates the value of genomic profiling in the evaluation and ultimate classification of brain tumors and that targetable genetic alterations are frequently detected in these tumors.

1847 Histologic changes induced by traditional and micropulse transscleral cyclophotocoagulation

Melike Pekmezci, Kareem Moussa, Behzad Amoozgar, Max Feinstein, Michele Bloomer, Ying Han. Univ. of California, San Francisco, San Francisco, CA

Background: Glaucoma is the leading cause of irreversible blindness in the world and lowering of intraocular pressure (IOP) via topical medications, laser or surgery has been the main treatment. Transscleral cyclophotocoagulation (TCP) is a cyclodestructive procedure that lowers IOP presumably by directly damaging the ciliary body. Recently, a modified application of TCP, known as micropulse TCP (MPTCP) was introduced, with potentially lower side effects. The histopathologic effects of MPTCP have not been described. The purpose of this study is to report the histologic changes of TCP and MPTCP treatment in cadaver eyes.

Design: Three pairs of adult eyes were obtained from eyebank, and superior and inferior halves were randomly assigned to TCP, single MPTCP, double MPTCP or control. Upon fixation, globes were examined under dissecting scope. Anterior halves of the globes were serially sectioned in the vertical axis into 3-5 slices. 12-15 step sections were examined for all tissue slices. Histologic features, scored as present or absent in each step section includes: 1- Split (between pigmented and nonpigmented epithelium), 2- Separation (of pigmented epithelium from stroma), 3- Coagulation (of collagen and destruction ciliary body stroma), 4- Destruction (of ciliary body epithelium). Discrete variables were compared using 4x2 Fisher's Exact test and logistic regression.

Results: 498 step sections of 46 tissue slices were examined. Changes were present only in some of the step sections of each tissue slice, and were limited to the pars plana. Table1 summarizes the distribution of findings. Separation and destruction of the epithelium were seen in TCP treated regions (p<0.001) while split was seen in all regions including the control. Stromal coagulation was more common in TCP-, but was also seen in single and double MPTCP-treated regions. In a model adjusted for clustering of findings in step sections of the single tissue slice, TCP was more likely to show stromal coagulation

than control (p=0.002); however, single or double MPTCP was not significantly different than control (p=0.35 and p=0.50).

Distribution of Histologic Features

		Control	TCP	MPTCP x1	MPTCP x2	p
Split	sections	35.3%	58.8%	41.2%	52.9%	0.166
	levels	19.1%	19%	11.1%	21.2%	0.849
Separation	sections	0	41.2%	0	5.9%	<0.001
	levels	0	9.2%	0	1.7%	0.004
Stromal Coagulation	sections	5.9%	76.5%	17.6%	17.6%	<0.001
	levels	2.7%	40.5%	7.7%	5.9%	0.002
Epithelial Destruction	sections	0	23.5%	0	0	<0.001
	levels	0	9.2%	0	0	0.032

Conclusions: Stromal coagulation changes seem to be present in the regions treated with MPTCP to a lesser extent than the regions treated with TCP. On the other hand, epithelial separation and destruction was almost exclusive to TCP-treated regions. Additional in vivo studies are required to assess whether these changes correspond with the lowering of IOP and/or with side effects such as inflammation.

1848 A Meta-Analysis of H3K27M Mutations In Gliomas Demonstrates Differential Location-Dependent Prognostic Outcomes

Drew W Pratt¹, Siva Kumar Natarajan², Adam Banda², Martha Quezado³, Pankaj Vats², Carl Koschmann², Rajen Mody¹, Arul Chinnaiyan⁴, Rishi Lulla⁵, Amanda Saratsis⁵, Sriram Vennet². ¹University of Michigan, Ann Arbor, MI, ²University of Michigan, ³NIH, Bethesda, MD, ⁴Plymouth, MI, ⁵Ann & Robert H. Lurie Children's Hospital of Chicago

Background: H3K27M mutant diffuse midline gliomas are a new WHO entity and are currently defined based on their infiltrative nature and their occurrence in midline structures. These tumors are associated with a dismal prognosis regardless of histologic grade and are therefore designated as WHO grade IV tumors. More recently, H3K27M mutations have been reported in rare non-infiltrating low-grade tumors and non-midline gliomas associated with or without an accompanying midline mass. The prognostic significance of H3K27M mutations in these tumors is not known. Moreover, there are conflicting data regarding the prognostic significance of H3K27M mutations in non-brainstem locations possibly due to relatively low sample sizes.

Design: To address these issues we performed a meta analysis from a total of 2,096 cases (H3K27M, n=1,036; WT, n=1,060) assembled from 74 studies (n=1,549), the cancer genome atlas (TCGA; n=260), and collaborative efforts (n=323).

Results: Across all tumor types and locations, overall survival (OS) was significantly shorter in H3K27M-mutated (n=500, median OS: 12.5) compared to H3WT tumors (n=595, median OS: 22) ($\chi^2=112.688$, log-rank, p<0.001). Adjusting for grade, H3K27M vs H3WT showed significantly shorter OS in H3K27M brainstem (K27M, n=123; WT, n=32; $\chi^2=4.810$, log-rank, p=0.028) and non-midline location tumors (K27M, n=15; WT, n=183; $\chi^2=4.505$, log-rank, p=0.034). H3K27M vs H3WT OS comparisons within thalamic (K27M, n=78; WT, n=58) and cerebellar tumors (K27M, n=11; WT, n=39) were not significantly different. Circumscribed (localized) H3K27M gliomas (n=23) had significantly shorter OS than WT (n=68) ($\chi^2=6.722$, log-rank, p=0.010). In subgroup analysis of location, OS was significantly different in H3K27M tumors: brainstem (median OS: 11.8) vs. thalamus (median OS: 13.5) ($\chi^2=7.708$, log-rank, p=0.005) and brainstem vs. non-midline (cerebral hemispheres) (median OS: 15) ($\chi^2=5.008$, log-rank, p=0.025). All other comparisons of OS by location were not significantly different. Infratentorial H3K27M tumors had significantly worse OS (median OS: 11.8) than supratentorial tumors as a whole (median OS: 14) ($\chi^2=8.437$, log-rank, p=0.004).

Conclusions: In summary, H3K27M mutations were associated with a significantly worse prognosis compared to H3WT in brainstem, non-midline and non-infiltrating gliomas.

1849 Alternative lengthening of telomeres, ATRX loss and H3 p.K27M mutations in Anaplastic Pilocytic Astrocytoma

Fausto Rodriguez¹, Jacqueline Brosnan-Cashman², Maria Adelita Vizcaino Villalobos³, Caterina Giannini⁴, Sandra Camelo-Piragua⁵, Milad Webb⁶, Marcus Matsushita⁷, Nitin Wadhwan⁸, Abeer Tabbarah⁹, Alicia Rodriguez-Velasco¹⁰, Christopher M Heaphy¹¹. ¹Johns Hopkins Univ, Baltimore, MD, ²Johns Hopkins University, ³Johns Hopkins University, Baltimore, MD, ⁴Mayo Clinic, Rochester, MN, ⁵University

of Michigan, Ann Arbor, MI, ⁶Ann Arbor, MI, ⁷Barretos, SP, Brazil, ⁸Lurie Children's Hospital, Chicago, IL, ⁹American University of Beirut, Beirut, NA, ¹⁰Hospital de Pediatria IMSS CMN S XXI, Mexico, Ciudad de Mexico, ¹¹Johns Hopkins University School of Medicine, Baltimore, MD

Background: Pilocytic astrocytomas (PA) are WHO grade I tumors typically occurring in children and young adults with excellent outcomes after surgical resection. Anaplastic changes in the form of brisk mitotic activity (with or without necrosis) may develop in a small subset and be associated with an aggressive behavior. The biologic features associated with this phenomenon are still unclear

Design: A total of 34 patients (23 M, 11 F) with a mean age of diagnosis of anaplasia of 33 years (range 3-75) were included in the study. Cerebellum/posterior fossa location was most common (n=21), followed by supratentorial hemispheric (n=5), supratentorial intraventricular (n=3), tectum/pineal (n=2), spinal cord (n=2) and brain NOS (n=1). Clinical and demographic characteristics including NF1 status were abstracted from retrospective chart review. A clinical diagnosis of NF1 (or *NF1* gene mutation) was present in 8 (24%). Alternative lengthening of telomeres (ALT) was tested using telomere specific FISH. A combination of immunohistochemistry, DNA sequencing and FISH were used to study *BRAF*, *ATRX*, p16, mutant IDH1 p.R132H and H3 p.K27M proteins.

Results: ALT was present in 20 (70%) cases and *ATRX* loss in 19 (61%), mostly in association (24 of 27, 89%). Discrepant results included ALT+/ATRX+ in 2 cases and ALT-/ATRX- in a single case with *ATRX* loss that was considered partial (i.e. present only in a subset of neoplastic cells). H3 p.K27M was present in 5 of 30 (17%) cases tested, 4 with concurrent *ATRX* loss and ALT. In 8 cases, ALT and/or *ATRX* was tested in the low grade PA component/precursor as well as the anaplastic PA. ALT/*ATRX* loss was present in both low grade and anaplastic components in 4 (of 5) cases, and was limited to the malignant component in a single case.

Conclusions: ALT and *ATRX* loss are frequent in anaplastic PA at the time of development of anaplasia or their precursors. Additionally, a small subset of anaplastic PA have H3 p.K27M mutations. These findings further support the concept that anaplastic PA is a distinct neoplasm with combined alterations typical of PA and diffuse gliomas.

1850 Mesenchymal neoplasms of the pineal region: a case series and literature review

Mary Rosenblatt, Randy D'Amico, Richard A Hickman, Peter B Wu, Jeffrey Bruce, Peter Canoll, George Zanazzi. Columbia University Medical Center, New York, NY

Background: Resected lesions from the pineal region are rare specimens encountered by the surgical pathologist, and the heterogeneity of these lesions can pose significant diagnostic challenges.

Design: The neuropathology and neurosurgery databases at our institution were searched for all cases of pineal region lesions resected between 1981 and 2017.

Results: A total of 360 lesions were identified in this predominantly adult cohort of patients. These included 91 pineal parenchymal tumors (25.2%), 90 glial tumors (25.0%), 83 germ cell tumors (23.1%), 27 pineal cysts (7.5%), 22 meningiomas (6.1%), 17 miscellaneous benign specimens (4.7%), 12 mesenchymal neoplasms (3.3%), 7 miscellaneous malignant lesions (1.9%), 6 glioneuronal tumors (1.7%), and 5 metastases (1.4%). The mesenchymal neoplasms included five solitary fibrous tumors (SFT)/hemangiopericytomas, two epithelioid hemangiioendotheliomas, two lipomas, one hemangioblastoma, one malignant spindle cell neoplasm, and one sarcoma. Recurrence occurred in two patients with SFT/hemangiopericytoma and in the patient with an epithelioid hemangiioendothelioma. A review of the literature expands the spectrum of mesenchymal neoplasms of the pineal region to include rhabdomyosarcoma, myxoid chondrosarcoma, osteosarcoma, angiosarcoma, and fibrosarcoma.

Conclusions: Although mesenchymal neoplasia within the pineal region is very rare, it is an important neoplastic subgroup that warrants consideration in the differential diagnosis of pineal region masses.

1851 Whole Genome Duplication and Chromothripsis in Adult Primary Glioblastomas

Audrey Rousseau¹, Frédéric Dugay², Marc-Antoine Belaud-Rotureau³, Philippe Mene⁴, Philippe Guardiola⁴, Blandine Boisselier⁴. ¹Angers, ²Rennes University Hospital, ³Universitary Hospital, Rennes, France, ⁴Angers University Hospital

Background: Glioblastoma (GBM) is the most frequent and lethal form of diffuse glioma. GBM displays chromosome (chr) instability (CIN) and recurrent somatic copy number alterations (SCNA). Recently, two distinct genetic events have been identified in cancer patients: whole genome duplication (WGD) and chromothripsis (CT). Such events have not been well described in large GBM cohorts. These events may contribute to tumor genesis/progression and gene

rearrangements.

Design: We used pan-genomic single nucleotide polymorphism (SNP) arrays to identify and characterize CT and WGD in 123 primary GBM. GAP (R package) was used to call somatic regions of copy number changes (CN) and determine the ploidy pattern for each tumor. The calling of CN changes was based on the analysis of logR and allelic ratios. WGD and CT were validated using, respectively, FISH technique and CTLPScanner, a web interface.

Results: CT occurred in 29.3 % of GBM (36/123) and mostly affected chrs 7, 9 and 12 (41.6%, 38.9%, and 4% of CT cases, respectively), with amplification of oncogenes (e.g., *EGFR* (chr 7), *MDM2/CDK4* (chr 12)), and homozygous deletion of tumor suppressor genes (e.g., *CDKN2A* (chr 9)). WGD was detected in 11.4% of GBM (14/123). Losses were seldom associated with LOH in WGD GBM suggesting genome doubling is an early genetic event. However, it occurred after the recurrent SCNA (e.g., chr 10 and 9p losses) observed in diffuse high-grade gliomas. WGD was observed in both initial and corresponding recurrent tumors. GBM with WGD were more aneuploid compared to GBM without WGD ($p < 0.0001$) suggesting genome doubling facilitates CIN. WGD GBM tended to occur at a younger age compared to near-diploid GBM (55 years vs. 63 years, respectively; not statistically significant). There was no significant association between CT or WGD occurrence and overall survival.

Conclusions: We identified CT and WGD in 29.3% and 11.4% of primary GBM, respectively. CT recurrently targets oncogenes and tumor suppressor genes known to be key players in gliomagenesis and tumor progression. The occurrence of CT points to underlying gene rearrangements (e.g., gene fusions), potential therapeutic targets in GBM. WGD is an early genetic event; it leads to CIN and aneuploidy. Such aneuploidy increases genetic variation and adaptive potential to a new or changing environment. Tumor cells with WGD may become resistant to radiation therapy and chemotherapy; hence give rise to tumor recurrence.

1852 A Single Center Study of Lymphomas and Reactive Infiltrates Involving the Conjunctival Mucosa: An Anatomically Unusual Site

Peyman Samghabadi¹, Edward Plowey², Robert Ohgam³. ¹Stanford Hospital and Clinics, Belmont, CA, ²Stanford Hospital and Clinics, Stanford, CA, ³Stanford University, Stanford, CA

Background: The diagnosis of lymphoma in the conjunctiva requires a combination of morphologic, immunophenotypic, molecular and cytogenetic analyses. However the frequency of types of lymphoma, morphologic patterns of involvement, and immunophenotypic and molecular features of lymphomas and reactive infiltrates in this site are poorly characterized.

Design: We performed a retrospective search of our pathology archives from 1995-2017 to identify lymphomas and reactive lymphoid infiltrates involving the conjunctiva. We evaluated the frequency and subtypes of different lymphomas, and studied the morphologic, immunophenotypic, molecular and cytogenetic features of lymphomas and reactive infiltrates involving the conjunctiva. We additionally studied associated clinical features.

Results: 183 biopsies with lymphoid infiltrates were identified. 98 were lymphomas and 85 were reactive infiltrates. The majority of lymphomas involving the conjunctiva were marginal zone lymphomas (MZL; 73/98) and follicular lymphoma (FL; 12/98) and to a lesser degree mantle cell lymphoma (MCL; 8/98). Interestingly, clinically localized FL of the conjunctiva is always low grade (10/10), and typically positive for BCL2 protein expression (8/10) though when evaluated, cases were negative by FISH for the *BCL2* translocation (0/4). One systemic follicular lymphoma involving the conjunctiva was seen and showed grade 3A morphology. Mantle cell lymphomas involving the conjunctiva were systemic and never localized cases. Finally, our review of reactive infiltrates involving the conjunctiva suggests that reactive intraepithelial B-cell infiltrates are not uncommon.

Table: Types of lymphomas involving conjunctiva

Lymphomas	N=98
Marginal zone lymphoma	73/98 (74%)
Follicular lymphoma	12/98 (12%)
Grade 3A	1/12 (1%)
Low Grade 1-2	11/12
Mantle cell lymphoma	8/98 (8%)
Diffuse large B-cell lymphoma	2/98 (2%)
NK/T-cell lymphoma	1/98 (1%)
Burkitt lymphoma	1/98 (1%)
Plasma cell neoplasm	1/98 (1%)

Conclusions: While MZL is the most common conjunctival lymphoma (74%), FL (12%) and MCL (8%) are not infrequent occurrences. FL localized to the conjunctiva, though frequently

BCL2 protein positive, does not typically show BCL2 translocations. Intraepithelial B-cell infiltrates should not be taken as definitive evidence of B-cell lymphoma.

1853 Estrogen Receptor Expression in Uveal Melanoma and Possible Prognostic Significance

Lynn Schoenfield¹, Caroline M Craven¹, Mohamed Abdel-Rahman¹, Colleen Cebulla¹. ¹The Ohio State University Wexner Medical Center, Columbus, OH

Background: Older reports have not demonstrated estrogen receptor (ER) expression in uveal melanoma (UVM). However, this tumor has been shown to harbor ER by immunohistochemistry (IHC), as previously presented at USCAP, as well as recent molecular studies; and it may impact prognosis and offer a target for therapy. The influence of gender on the prognosis of uveal melanoma has historically been considered insignificant; but in recent years, data has emerged suggesting that there are differences between men and women. The purpose of this study is to confirm that estrogen receptors (ER) are present in a subset of uveal melanomas and to determine whether ER expression impacts patient outcome (metastasis or death) or relates to known genetic high risk features.

Design: Incidence and outcome data of 50 cases (47 patients) of UVM from 2010-17 were analyzed. The study was approved by the Ohio State University Wexner Medical Center IRB. Of the 50 cases, there were 41 enucleations, 3 iris excisions, 1 iridociliary excision, 1 choroid biopsy in a case of known liver metastasis, and 2 liver metastases. They were stained for ER by IHC using a brown chromogen. Cases were considered positive if at least 1% of the tumor nuclei stained and were scored by one ocular surgical pathologist who also has had extensive experience in breast pathology. Chromosome 3 and 8q status was determined by cytogenetics and/or FISH; in some cases, gene expression profiling (GEP) was also available. Patient outcome was obtained from the electronic medical record.

Results: Follow-up ranged from < 1-86 months. There were 28 men (60%) and 19 women (40%). Six (13%) patients were known to be DOD, 4 (67%) of them men; 9 (19%) had established metastases, 6 (67%) of them men. ER was positive in 26 cases (52%) from 24 (51%) of patients: 17 cases (65%) were from men. In 3 cases in which both primary and metastasis were available, there was ER concordance (ER positive in both for 2 patients and negative in both for 1 patient). 24 patients (51% total, 15 or 63% of which were men) had high risk genetic features (monosomy 3, 8q gain, or Class 2 GEP). Comparing IHC results for ER to outcome showed: 3 of 4 men who died were ER positive and 0 of 2 women who died had positive ER. For metastases, 5 of 6 men (83%) and 2 of 3 women (67%) were positive for ER. Of the 24 ER negative cases, only 4 (17%) had a negative outcome.

Conclusions: Gender and ER expression may play a role in the incidence and behavior of UVM and warrants further study.

1854 Molecular Characteristics of Gliosarcomas

Nima Sharifai, Samantha McNulty, Sonika Dahiya. Washington University in St. Louis, Saint Louis, MO

Background: Gliosarcoma (GS) is a rare subtype of glioblastoma (GBM) that features mesenchymal differentiation. Previous studies have found that GS shares many of the same molecular characteristics as GBM, and a subset of gliosarcomas possess abnormalities in the Wnt signaling pathway.

Design: We recently came across five gliosarcoma cases at our institute that underwent next generation sequencing. We further assessed copy number changes, chromosomal imbalances, and single nucleotide variations in these tumors.

Results: There were 3 male and 2 female patients (age 15-74, median 59 years). In three of the cases, the tumor was located in the temporal lobe at initial presentation. One case involved the frontal lobe, and another case localized to the thalamus and brainstem. Notable chromosomal alterations included losses on chromosomes 10 (5/5, 100%) and 9p (3/5, 60%), and gains on chromosome 7 (4/5, 80%). Two single nucleotide variations were noted in Wnt signaling pathway genes, *CSNK1A1* - chr5:149499672T>C and *CTNNB1* - chr3:g.41267276A>G, in 4/5 and 1/5 cases, respectively. The former variation involves the 3' untranslated region of the gene's transcript, while the latter variation causes a missense mutation in exon 7 of the beta-catenin gene. To our knowledge, the effects of these specific variants on transcript processing and protein functioning have not yet been elucidated.

Conclusions: Our results reinforce the notion that gliosarcoma and glioblastoma share many of the same molecular and cytogenetic features. Further investigation into the significance of Wnt signaling pathway alterations in the pathogenesis of gliosarcoma is of interest for its potential therapeutic implications.

1855 Lack of PD-1 and PD-L1 protein expression in pilocytic astrocytoma

Namita Sinha¹, Joanna Phillips², Ayca Ersen³, Tarik Tihan⁴, David Gutmann⁵, Sonika Dahiya⁶. ¹Washington University in St. Louis, St. Louis, MO, ²University of California, San Francisco, ³Izmir, Turkey, ⁴UCSF, San Francisco, CA, ⁵Washington University in St. Louis, ⁶Washington University in St. Louis, Saint Louis, MO

Background: Pilocytic astrocytoma (PA) is the most common benign brain tumor of childhood. Although most patients exhibit a benign course, a small subset of tumors recurs and demonstrate cerebrospinal fluid (CSF) dissemination. While *BRAF* alterations might act as therapeutic targets in such scenarios, there still remains a small subset of tumors that lack these alterations. Recently, the binding of PD-L1 to its receptor PD-1 has been shown to induce an immune escape mechanism and to play a critical role in tumor initiation and progression. Further, there is also an emerging role of immune cells (including microglia) in gliomagenesis. We investigated the role of common immune markers, PD-1, and PD-L1 in pilocytic astrocytomas.

Design: A tissue microarray containing 38 PA cases was prepared, and immunohistochemical analysis for CD3, CD20, CD21, CD68, CD163, Ki-67, PD-1, and PD-L1 was performed. The relationship between density of immune cells and Ki-67 proliferation index of the tumor was examined.

Results: Sparse-to-moderate density of tumor infiltrating lymphocytes was found in all PAs (CD3+ T cells varied from 0.4 to 17.6%, CD20+ B cells varied from 0.01 to 1.1%, and CD21+ dendritic cells comprised < 0.01% of tumor). All PAs had moderate to markedly high density of CD68 and CD163 positive tumor-associated microglial cells/macrophages (TAMs) as either scattered infiltrates and/or perivascular aggregates, comprising in some examples up to 49.4% of the tumor cells. TAMs comprising >10% of cells in 30 of 38 (79%), and 25 of 38 (66%) cases were CD163- and CD68-immunoreactive, respectively. Four of 38 PA cases (10.5%) had high Ki-67 proliferation indices of >5.0%. None of the 38 PA cases, including PAs with high proliferation index, showed any reactivity for PD1 or PD-L1.

Conclusions: TAMs comprise the largest population of immune cells within this cohort along-with a notable lack of PD-1 or PD-L1 protein expression, although small representation of tumor in tissue microarray is a caveat. While more studies are required to support this notion, our findings do raise a potential role of leveraging TAMs as a potential therapeutic target instead of check-point inhibitors.

1856 IDH1 Mutation Enhances Radiation Sensitivity by Regulating EMT and Apoptotic Pathway in Malignant Glioma

Mishie A Tanino, Arisa Kitazaki, Mei Kuzasa, Hirokazu Sugino, Yusuke Ishida, Lei Wang, Masumi Tsuda, Shinya Tanaka. Hokkaido University, Sapporo, Hokkaido

Background: Malignant glioma (MG) is one of the most aggressive neoplasms in human cancers. We have previously reported glial-mesenchymal transition (GMT) by increasing in snail expression after irradiation was related to radio-resistance in MG (Neuro-Oncol. 2014). Although MG with IDH1 mutation has been reported to show better prognosis compared to MG with IDH1 wild type, it has not been clarified how the IDH1 mutation affects radio-sensitivity in MG.

Design: To investigate the role of IDH1 mutation on radio-sensitivity, we first established IDH1^{WT} and IDH1^{R132H} overexpressing KMG4 and U87 MG cell lines using pCX4-puromycin-IDH^{WT} and pCX4-puromycin-IDH^{R132H} vectors and performed metabolome analysis by capillary electrophoresis-mass spectrometry. Second, to mimic irradiation therapy, we irradiated multi-fractionated 20 Gy to IDH1^{R132H} overexpressing MG cells (IDH^{R132H} MGs) and IDH1^{WT} overexpressing MG cells (IDH^{WT} MGs) and analyzed the apoptosis and EMT related molecules by immunoblotting and qRT-PCR. Lastly, we performed migration and invasion assays to evaluate malignant potentials.

Results: IDH^{R132H} MGs showed lower levels of α -KG, NADPH, reduced GSH and ATP, while higher levels of 2-HG, oxidized GCH, ADP and AMP compared to IDH^{WT} MGs. IDH^{R132H} MGs showed a decrease in the phosphorylation levels of AKT and Bcl2 expression compared to IDH^{WT} cells. In addition, IDH^{R132H} MGs showed an increase in phosphorylation levels of p53 and cleaved PARP expression. Although snail mRNA was increased after irradiation compared to before in IDH^{WT} MGs, it was not increased in IDH^{R132H} MGs after irradiation. Furthermore, both motility and invasiveness were increased after irradiation in IDH^{WT} MGs, however these phenomenon was not occurred in IDH^{R132H} MGs.

Conclusions: IDH1 mutation induces changes in metabolic status and may lead to radio-sensitivity by regulating apoptosis and GMT leading to better prognosis in MGs.

1857 Immunohistochemistry for NF- κ B Components Accurately Identifies RELA-Rearranged Ependymomas

Matthew Torre¹, Azra Ligon², Jason L Hornick², David Meredith².
¹Brookline, MA, ²Brigham and Women's Hospital, Boston, MA

Background: Histologic grading of ependymomas, a class of gliomas that can arise along the ventricular system and spinal cord, correlates poorly with patient outcome. Categorizing ependymomas by anatomic location (i.e. supratentorial, posterior fossa, or spinal cord) and by molecular subgroup appears to have greater prognostic value. Approximately 70% of supratentorial ependymomas contain *C11orf95-RELA* fusions, resulting in constitutively active NF- κ B signaling. *RELA*-rearranged ependymomas, generally diagnosed by molecular cytogenetic techniques or RT-PCR, are associated with significantly worse outcomes. In this study, we examine the utility of using immunohistochemical stains for cyclin D1, L1CAM, and p65 -- proteins involved in NF- κ B signaling pathways -- for detecting *RELA*-rearranged ependymomas.

Design: Immunohistochemistry for cyclin D1, L1CAM, and p65 was performed on sections of ependymomas from each anatomic location (supratentorial, n=17; posterior fossa, n=21; spinal cord, n=37), as well as several histologic mimics, including astroblastoma (n=2), gliomas with angiocentric architecture (n=6), and embryonal tumors (n=3). The staining profiles were correlated with array comparative genomics hybridization (aCGH) data, which were available for a subset of the cases.

Results: Evidence of *C11orf95-RELA* fusion was seen only in 4/5 supratentorial ependymomas for which microarray had been performed. Cyclin D1 was positive in 9/17 supratentorial ependymomas, including the 4 *RELA*-rearranged ependymomas, 1/21 posterior fossa ependymoma, and none of the spinal cord ependymomas, astroblastomas, gliomas with an angiocentric architecture, or embryonal tumors. L1CAM and p65 were positive in 8/17 supratentorial ependymomas, including all 4 *RELA*-rearranged ependymomas, and negative in all other tumors.

Conclusions: Molecular subgrouping of ependymomas is essential for predicting clinical outcome. Cyclin D1, L1CAM, and p65 immunohistochemistry is highly sensitive for identifying ependymomas with *RELA* rearrangements; however, L1CAM and p65 show greater specificity. Routine use of these immunostains in the workup of supratentorial ependymomas could provide a cost-effective initial step in an algorithm to identify tumors with *RELA* rearrangements.

1858 Genome-wide Methylation Profiling of Low-grade and Anaplastic Pleomorphic Xanthoastrocytoma

Rachael A Vaubel¹, Paul Decker², Alissa Caron², Jeanette Eckel-Passow², Amulya NageswaraRao², Fausto Rodriguez², Robert Jenkins⁴, Caterina Giannini⁴.
¹Mayo Clinic, Rochester, MN, ²Mayo Clinic, ³Johns Hopkins Univ, Baltimore, MD, ⁴Mayo Clinic, Rochester, MN

Background: Pleomorphic xanthoastrocytoma (PXA) is a rare astrocytic neoplasm predominantly affecting children and young adults. The 2016 *WHO Classification of Tumors of the Central Nervous System* recognizes PXA (WHO grade II) and anaplastic PXA (A-PXA, WHO grade III) as distinct entities, with A-PXA defined by the presence of >5 mitoses per 10 high power fields. PXA is characterized by BRAF V600E mutation (~60% of tumors) and homozygous deletion of *CDKN2A/B* (up to 90% of tumors). However, the genetic and epigenetic alterations underlying PXA without BRAF V600E mutation as well as the genetic determinants of histologic grade and aggressive behavior are poorly defined.

Design: DNA was extracted from FFPE material and the Illumina Methylation EPIC array was performed on 35 PXA (18 PXA, WHO grade II and 17 A-PXA, grade III). BRAF V600E was assessed by immunohistochemistry and sequencing and was mutated in 23 (66%) tumors: 78% PXA and 53% A-PXA. Unsupervised hierarchical clustering was performed using the 10000 most variable probes; Pearson correlation was used for the distance metric. Differential methylation analysis was performed using a modified t-test; probes with p-values <10⁻⁷ were considered statistically significant.

Results: Unsupervised clustering data did not distinguish PXA from A-PXA nor did it reflect BRAF V600E mutation status. Comparison of PXA and A-PXA identified 21 probes with significant differential methylation, 10 hypermethylated and 11 hypomethylated in A-PXA. Differentially methylated probes included the promoter regions of genes involved in cell division, hypoxia, and vasculogenesis. Comparison of BRAF V600E mutant and non-mutant tumors identified no significantly differentially methylated probes.

Conclusions: Genome wide methylation identified 21 probes differentially methylated in anaplastic PXA. Further validation is needed to confirm this finding and the role of these epigenetic changes in anaplasia and aggressive behavior in PXA.

1859 IDH-Wildtype Glioblastomas with Chromosome 19/20 Co-Gain: A Study of Genomic Associations for this Prognostically Important Subset

Jose Velázquez Vega¹, Jennifer Hauenstein², Debra Saxe³, Lindsey Lowder⁴, Matthew J Schniederjan⁴, Daniel Braš⁵, Stewart Neill⁶.
¹Emory, ²Emory University, ³Emory University School of Medicine, Atlanta, GA, ⁴Emory University School of Medicine, ⁵Northwestern University Feinberg School of Medicine, Chicago, IL, ⁶Emory Univ/Medicine, Decatur, GA

Background: Long term survival in *IDH*-wildtype (wt) glioblastoma (GBM) is a rare event. A significant proportion of long term survivors in the pre-*IDH* era literature are probably now recognized as *IDH*-mutant GBMs. However, a recent study identified a clinically relevant subgroup of *IDH*-wt GBM with chromosome 19/20 co-gain that had a more favorable outcome. Segmental gains of either chromosome are not rare in high grade astrocytoma, however the co-gain has an estimated frequency of less than 20% and has been associated with better overall survival.

Design: We performed a search of our institutional database for cases of *IDH*-wt GBM with whole chromosomal co-gains of 19 and 20. Partial and segmental gains were not included. We assessed clinical information from the electronic medical record and tabulated the immunohistochemistry (IHC) results and copy number alterations (CNA) with a cytogenomic molecular inversion probe (MIP) array.

Results: We identified 12 primary *IDH*-wt GBMs occurring in 7 males and 5 females with age at diagnosis ranging from 35-75 years (59.3 ± 11.6 years). Imaging findings showed hemispheric tumors with high grade features that ranged in size from 1.3-6.2 cm. Most tumors were subtotally resected and treated with standard of care adjuvant chemoradiation. Follow up ranged from 1-43 months, with only one patient followed beyond 3 years after initial diagnosis. All tumors met histologic criteria for GBM and were *IDH*-wt (IHC and sequencing analysis). ATRX IHC highlighted intact nuclear expression in all cases and p53 overexpression was noted in 7 cases by IHC. All tumors had the classic +7/-10 CNA (mostly whole chromosomal) and 9 had loss of *CDKN2A/B* (mostly homozygous). Amplification events were common: 6 tumors had *EGFR*, 3 had *CDK4*, 2 had *MYC*, and 2 had *MDM2* amplifications, some co-occurring.

Conclusions: Chromosome 19/20 co-gain has been identified as a possible biomarker of prognostic significance within *IDH*-wt GBMs. The co-occurrence arises in the setting of quintessential genomic alterations of *IDH*-wt astrocytomas such as +7/-10, *CDKN2A/B* loss and focal amplifications including *EGFR*. Further studies that include longer follow up are necessary to further elucidate the nature and possible underpinnings of the survival advantage.

1860 Hippocampal injury in the setting of Alzheimer's disease

Jeffrey Whitman¹, Hamza Coban², Harry Vinters³.
¹University of California, San Francisco, San Francisco, CA, ²UCLA Medical Center, ³UCLA Medical Center, Los Angeles, CA

Background: The separation of Alzheimer's disease (AD) and vascular dementia (VaD) has been questioned, considering that the pathologic lesions characteristic of both entities are often present in the brains of the elderly. The primary etiology of these lesions and their role in cognitive impairment are neither well understood nor well-described at the neuroanatomical level. In this study, we characterize patterns of vascular injury and neurodegenerative burden in the hippocampus in the setting of AD. By focusing attention on this region, we hope to provide evidence to the role of hippocampal injury in the AD/VaD spectrum.

Design: Autopsy cases with a neuropathologic diagnosis of AD were retrospectively reviewed for hippocampal injury, including hippocampal sclerosis and hippocampal microinfarcts. Histology was performed from stored tissue blocks and new sections made from banked tissue. Immunohistochemistry for glial fibrillary acidic protein (GFAP), ionizing calcium binding adaptor molecule 1 (Iba1) and TAR DNA binding protein 43 (TDP-43) were performed on cases to evaluate astrocytes, microglia, and proteinopathy-associated neuronal intracytoplasmic inclusions (NCl), respectively.

Results: A total of 249 AD cases were reviewed; 83.5% (n=208) being pure AD and 16.5% (n=41) being mixed AD (comorbid with another dementing disorder). Seventy-four brains (29.8%) showed neuropathologic features of AD and hippocampal injury. Hippocampal sclerosis (HS) was the most common lesion, seen in 58 (23.4%) cases. Hippocampal microinfarcts (HM) were identified in 16 (6.5%) cases. HS had slight bilateral predominance (53.4%), while HM were more commonly unilateral (81.2%).

AD/HI cases with banked tissue were assessed for additional hippocampal injury. Of 9 cases reviewed, 4 showed more extensive HI with additional sampling, suggesting that limited dementia protocols could miss a significant amount of HI.

AD patients with HI were, on average, older at age of passing than those without these lesions (85.6 vs. 80.2 years; p<0.01), but did not

demonstrate a statistically significant difference in AD severity as measured by Braak and Braak scoring (5.39 ± 0.87 vs. 5.38 ± 0.95) nor neurodegenerative HS pathology by TDP-43 staining.

Table 1. Demographics of AD cases stratified by etiology of dementia and HI: *p= 0.0005 compared to AD without HI. Abbreviations: Alzheimer's disease (AD), Hippocampal Injury (HI).

	Age (years)	% Female (n)	Braak & Braak	Brain Wgt (g)
Total AD	81.6 ± 10.7	54.9% (140)	5.4 ± 0.9	1144 ± 168
Pure AD	81.5 ± 11.1	55.6% (114)	5.4 ± 0.9	1140 ± 171
Mixed AD	82.1 ± 11.2	55.1% (27)	5.2 ± 0.8	1165 ± 163
AD w/ HI	85.5 ± 9.9*	58.9% (43)	5.3 ± 0.9	1113 ± 166
AD w/o HI	80.2 ± 10.6	55.9% (85)	5.3 ± 0.9	1156 ± 165

Conclusions: Our study was able to report findings of hippocampal injury in the spectrum of AD. This study's conclusions are novel for their relation to clinical characterization and reveal significant associations with increased age over neurodegenerative pathology in AD.

1861 PREVIOUSLY PUBLISHED

1862 Orbital involvement by aggressive hematopoietic neoplasms

Xiao Yi Zhou¹, Kirtee Raparia², Juehua Gao³, Yi-Hua Chen⁴.
¹Northwestern Memorial Hospital, Chicago, IL, ²Northwestern University, Chicago, IL, ³Northwestern Memorial Hosp., Chicago, IL, ⁴Northwestern University, Chicago, IL

Background: The most common lymphoma involving the orbit is the extranodal marginal zone lymphoma of mucosa-associated lymphoid-associated tissue (MALT lymphoma). The data on orbital involvement by aggressive hematopoietic neoplasms are relatively limited.

Design: Patients with orbital involvement by lymphoma/leukemia between 2002 and 2015 were searched from Pathology database at Northwestern Memorial Hospital. The biopsy slides, ancillary studies and clinical findings were reviewed.

Results: Of 46 cases of lymphoma/leukemia involving the orbit, 39 were low-grade lymphomas including 30 MALT lymphomas, and 7 were aggressive hematopoietic neoplasms including five diffuse large B-cell lymphomas, one myeloid sarcoma and one acute B-lymphoblastic leukemia. The clinical presentations included vision loss, diplopia and photopsia. Of particular interest, the orbital mass was the initial presentation of a high-grade, triple-hit lymphoma transformed from a systemic, low-grade follicular lymphoma without any clinical or laboratory findings suggestive of transformation. In another case, the orbital mass was the only manifestation of a relapsed acute leukemia of mixed lineage after six years in remission.

Conclusions: The orbit can be involved by a variety of aggressive hematopoietic neoplasms and could be the initial site of disease progression or relapse. A prompt diagnosis is critical for appropriate treatment.